

# **SIMULATION-BASED STUDY OF HIGH PERFORMANCE DOUBLE GATED FD-SOI TRANSISTOR FOR pH SENSING APPLICATIONS**

*A thesis is submitted*

*by*

**NAVEEN KUMAR**

**2017PEV5175**

*Under the guidance of*

**Dr. C. PERIASAMY**

*In partial fulfilment for the award of the degree of*

**MASTER OF TECHNOLOGY**

*to the*

**DEPARTMENT OF ELECTRONICS AND  
COMMUNICATION ENGINEERING**



**Electronics and Communication Engineering Department**

**Malaviya National Institute of Technology, Jaipur**

**JULY, 2019**



**DEPARTMENT OF ELECTRONICS AND  
COMMUNICATION ENGINEERING  
MALAVIYA NATIONAL INSTITUTE OF TECHNOLOGY  
JAIPUR-302017, RAJASTHAN, INDIA**

---

## **CERTIFICATE**

This is to certify that the Dissertation Report entitled “**Simulation Based Study of High Performance Double gated FD-SOI transistor for pH sensing applications**” by **Naveen Kumar** is the work completed under my supervision and guidance, hence approved for submission in partial fulfillment for the award of degree of Master of Technology in VLSI to the Department of Electronics and Communication Engineering, Malaviya National Institute of Technology, Jaipur in the academic session 2018-2019 for full time post-graduation program of 2017-2019.

**Date:**

**Place:**

**Dr. C.Periasamy**  
**Assistant Professor**  
**(Project Supervisor)**  
**Dept. of Electronics and**  
**Communication Engineering**  
**MNIT Jaipur 302017**



**Department of Electronics and Communication Engineering  
Malaviya National Institute of Technology, Jaipur**

---

**DECLARATION**

I declare that,

- a) The work contained in this dissertation is original and has been done by me under the guidance of my supervisor.
- b) The work has not been submitted to any other institute for any degree or diploma.
- c) I have followed the guidelines provided by the institute in preparing the dissertation.
- d) I have conformed to the norms and guidelines given in the Ethical code of conduct of the institute.

**Date:**

**Naveen Kumar  
(2017PEV5175)**

# ACKNOWLEDGEMENT

---

I take this opportunity to express my deep sense of gratitude and respect towards my supervisor of the Dissertation, **Dr. C.Periasamy**, Assistant Professor, Department of Electronics & Communication Engineering, Malaviya National Institute of Technology. I am very much indebted to her for the generosity, expertise and guidance I have received from her while working on this project and throughout my studies. Without her support and timely guidance, the completion of my project would have seemed a far-fetched dream. In this respect, I find myself lucky to have her as my Project guide. he has guided me not only with the subject matter, but also taught me the proper style and techniques of working.

I would also like to thank **Prof. D. Boolchandani**, Professor of Electronics & Communication Engineering Department for his co-operation and help rendered in numerous ways for the successful completion of this work.

**Naveen Kumar**  
**(2017PEV5175)**

## Abstract

ISFET's are derived versions of MOSFET's (Metal Oxide Semiconductor Field Effect Transistors) where the gate electrode is replaced by a reference electrode and an electrolyte. In spite of the advantages like compatibility with standard CMOS process technologies, precise process control, operability at equilibrium conditions, capability for label free detection and ease of disposability these devices suffer from few inherent weaknesses. They are unreliable and unstable due to ionic damages in case of long term use. The sensing principle includes variation in surface potential due to ionic interactions at the electrolyte/gate oxide interface. One limitation of the ISFET based sensors which has gained huge research focus in the past decades is the poor sensing margin within the Nernstian limit (59 mV per pH) at room temperature. This work focuses on improving the threshold voltage sensitivity to 12-15 times the Nernstian limit.

This work reports realization of pH sensitivity beyond the Nernstian limit using a double gated (DG) ISFET based FDSOI on Si (silicon) and SiGe (silicon germanium) channel. Different dielectrics have also been used in the work in order to analyze their impact on device sensitivity. Device has been simulated using  $\text{SiO}_2$ ,  $\text{Si}_3\text{N}_4$  and  $\text{Al}_2\text{O}_3$  as gate dielectric and the device sensitivities have been compared. High speed, low power consumption and low leakage currents are among some inherent advantages of FDSOI. The DG ISFETs make use of the back gate and reference electrodes in order to effectively control the biasing conditions. Whereas in SG-ISFET's (Single Gated), the reference electrode aids the electrostatic coupling of the electrolyte potential to the transistor channel. Deliverables through this work include a high pH sensitive FDSOI's on Si and SiGe substrates with sensitivities above Nernstian limit, a comparative analysis of impact of different gate dielectrics on device sensitivity, the best performing gate dielectric for dedicated pH sensing application.  $\text{Al}_2\text{O}_3$  based FDSOI on SiGe exhibits the best performance with high sensitivity of 760mV/pH .

## List of Tables

4.1	Parameters of Different Oxides	26
4.2	Device Dimensions	26

## Abbreviations

$V_{TH}$	Threshold Voltage
$V_{DD}$	Supply Voltage
$I_{ON}$	On State Current
$I_{OFF}$	Off State Current
$C_{GS}$	Gate Capacitance
$K$	Boltzmann Constant
$T$	Temperature
$Q$	Carrier Charge
$I_{DS}$	Drain to Source Current
$C_L$	Load Capacitance
$T_{OX}$	Oxide Thickness
$I_{LEAK}$	Leakage Current
$T_{SI}$	Silicon Thickness

## List of Figures

1.1	Conventional MOSFET structure	4
1.2	$I_D$ versus $V_{GS}$ characteristics of MOSFET	5
1.3	Structure of FDSOI	7
3.1	Atlas device simulator	16
3.2	Meshing in the Structure	17
4.1	Different types of SOI MOSFET structures	24
4.2	Device Structure	25
4.3	Channel doping	26
4.4	Simulated Structure	27
4.5	Variation of density of states of conduction band	28
5.1	Threshold voltage shift with pH immobilization	31
5.2	pH Sensing characteristics for $\text{SiO}_2$	33
5.3	pH Sensing characteristics for $\text{Si}_3\text{N}_4$	34
5.4	pH Sensing characteristics for $\text{Al}_2\text{O}_3$	35
5.5	Comparison of device transfer and transconductance characteristics	36
5.6	pH Sensing characteristics for SiGe based Device	37
5.7	Sensitivity enhancement of proposed device over conventional Si based device	38
5.8	Impact of pH immobilization on device channel potential	39
5.9	Cut off frequency of the proposed SiGe based pH sensor	40

## Table of Contents

<b>1</b>	<b>INTRODUCTION</b>	<b>1</b>
1.1	Introduction and Motivation	1
1.2	Objective	2
1.3	Thesis Organization	2
<b>2</b>	<b>LITERATURE REVIEW</b>	<b>4</b>
2.1	MOSFET	4
2.2	Modes of Operation	5
2.3	Importance of Scaling	5
2.4	Innovations in MOS Technology	6
2.5	Limitations of MOSFET	6
2.6	FDSOI Transistor	7
2.6.1	Device Overview	7
2.6.2	Advantage and Disadvantage	8
2.7	Literature Survey	9
<b>3</b>	<b>SIMULATION</b>	<b>14</b>
3.1	Introduction	14
3.2	Steps for Defining Structure	17
3.3	Specification of Models	20
3.4	Commonly Used Models	20
3.5	Numerical Methods	21
3.6	Methods to Obtain Solutions	21
3.7	Prediction of Results	22
<b>4</b>	<b>DEVICE STRUCTURE AND OPERATION</b>	<b>23</b>
4.1	Different types of SOI MOSFETs	23
4.2	Device Structure	24
4.3	Device Working	27
4.4	Classification of Sensor	29
4.5	Types of Sensor in Electronics	30
<b>5</b>	<b>RESULTS AND DISCUSSION</b>	<b>31</b>
5.1	Impact of pH Immobilization on Device Threshold Voltage	31



5.2	pH Sensing Performance for various Oxides	32
5.2.1	SiO <sub>2</sub> as Oxide	33
5.2.2	Si <sub>3</sub> N <sub>4</sub> as Oxide	34
5.2.3	Al <sub>2</sub> O <sub>3</sub> as Oxide	45
5.3	Si versus SiGe	36
5.4	Results	37
5.4.1	Final FDOSI with Al <sub>2</sub> O <sub>3</sub> as Oxide	37
5.4.2	Sensitivity Comparison	38
5.5	Impact of pH Immobilization on Channel Potential	39
5.6	Device Cut off Frequency	40
<b>6</b>	<b>CONCLUSION AND FUTURE WORK</b>	<b>42</b>

**Introduction and Motivation**

With the modernization in technology processors were designed with efficient usage. Since past few decades, the MOSFETs are scaled down to increase more functionality in device and design a structure with the integration of more transistors on a single device. Certain conditions were provided by ITRS. Firstly the advancement of scaling includes less power consumption with more no. of transistors on a single chip and simulation of three dimensional structure. The second one includes the combination of heterogeneous technology and designing the new devices with the efficient way. With the introduction of new technology, the power consumption has increased. The devices which are best suited for low power consumption are CMOS with scaling of device on large scale. But the rate of increase in transistor is greater than the rate of increase in area due to scaling. As a result of which the temperature increases. This causes to increase in power dissipation of model. Various work has been done in the field of Sensing applications such as bio Sensor, pH Sensor, Enzyme based Sensor, Glucose Sensor etc. All sensors have their drawbacks with limited sensitivity. Sensors are based on different mechanisms. Some work on the principle of current change while some work on current change.

pH sensors might have different sensing mechanisms based on the device used. HEMT devices use current sensitivity while FDSOI use Threshold voltage sensitivity. Work has been done previously in sensitivity enhancements in the form of sensitivity. Various devices have been formed with varied materials in order to enhance the sensitivity. But the work done has only enhanced it to nearly 500 mV with single device. This sensitivity is not enough for very close pH measurements. For high grade pH sensors sensitivity increase has been demanded. This gap has motivated to further study in the field of pH sensors. Motivation also comes from better oxide selection since oxide affects the device performance in various aspects such better sensitivity and better control over leakage current. Oxide selection also affects the lifetime of device since pH measurement affects the oxide in contact.

## **Objective**

pH sensors can be used to detect the change in the hydrogen ion concentration for an aqueous solution. Electrolyte region can be simulated by replacing with the hole and electrons which can represent the ions regarding the aqueous pH solution. Effect of the pH change on various characteristics such as threshold voltage, surface potential, drain current and sensitivity can be studied. Here, change in the device threshold voltage may be defined as pH response as the value of pH is varied. pH value can be varied from acidic to basic which in turn shifts the current characteristics. Effect of various other parameters such as thickness of electrolyte and device dimensions has also been studied. Hence this work has focused mainly on sensitivity enhancement which is based on threshold voltage. Work has been done to increase sensitivity up to 760mV which is much more than that of 500mV. Until now industry has been focused only on current sensitivity, but with great sensitivity in threshold voltage a new device can be formed with a better alternative. Various oxides have been used for better results. Simulations have been done for SiO<sub>2</sub>, Si<sub>3</sub>N<sub>4</sub> and Al<sub>2</sub>O<sub>3</sub> with sensitivity measurements. Idea is to measure the sensitivity by varying the oxides as well as channel. Device dimensions can also act as an important parameter to improve the performance. Hence the device has to be designed with optimum dimensions in order to attain maximum probable results.

## **Thesis Organization**

Chapter One contains the introduction and motivation needed for the project. It includes a brief introduction of the previous and current work. Objective has also been discussed to briefly overview the work.

Chapter Two includes the background survey and literature review. CMOS journey has been discussed leading up to current devices such as TFET, Junctionless, FDSOI etc. FDSOI working and previous papers have been discussed along with the gap. Various sensors based papers have been discussed with their working and the concepts used. Papers have been briefly discussed with the essence and the working concept such as Gouy-Chapman theory has been discussed. Site binding charge concept simulation theory for pH sensing has been discussed.

Chapter Three include simulation methods and models used. Models have discussed briefly and various parts of Silvaco tool such as Deck Build, Tonyplot have been discussed. Meshing have been discussed along with various types. Chapter mainly include simulation methodology and various commands used .

Chapter Four describes the device structure and operation for FDSOI. It describes electrical characteristics for the device. Also device structure has been used along with sample structure. Comparison has been performed with previous work. Simulation method has been discussed and electrolyte simulation has been explained.

Chapter Five include results and discussion with output plots. Output plots have been derived for three different oxides with silicon as channel material. At last final device simulation has been done with SiGe as channel material. Device performance has been compared with previous devices. Device dimensions have also been discussed. At last device speed has been discussed in terms of cut off frequency analysis.

Chapter Six includes conclusion and future scope. Brief summary of conclusion has been given with output results. In future scope some gaps have been discussed which can be further improved.

## 2.1 MOSFET

MOSFETs are developed gradually from the MOS integrated circuit technology. MOSFET is a four terminal device which can be applied in analog and digital circuits. An Insulated layer of dielectric material which is  $\text{SiO}_2$  mainly is deposited over silicon substrate its structure is same as planar capacitance. There are four terminals gate, source, drain, and body in which body is connected to source hence making it four terminal device.

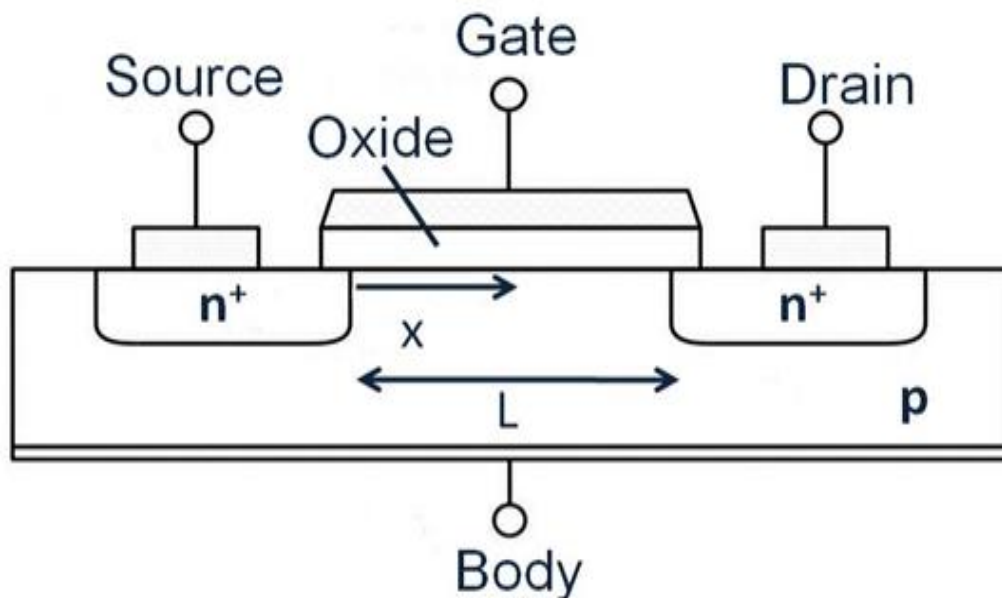


Figure 2.1 Conventional MOSFET structure[21]

*MOSFET structure:* The current flow is mainly supported by the electrons. Source and Drain regions are formed by using  $n^+$  regions. In enhancement mode, channel starts forming between source and drain. When sufficient positive voltage is applied between gate and source the holes are repelled which leads forming a channel with negative charges. As gate voltage further increased, electron density at the inversion layer increases and current flow from drain to source increases.

## 2.2 Modes of Operation

There are three modes of operation of MOSFET:

1) *cut off region*: If the applied gate voltage is kept lesser than the threshold voltage then Transistor is operated to be in off state and Drain current is zero because voltage is not sufficient to form the channel.

2) *linear or triode region*: If the applied voltage is kept greater than the threshold voltage, then drain and source has current flowing through it, also gate source voltage difference is more than drain to source voltage difference.

3) *Saturation region*: If gate to source voltage is exceeds the threshold voltage, and also drain to source voltage becomes greater than difference of gate to source voltage and threshold voltage then device goes into saturation region. In this mode, the MOSFET can behave as an ideal current source.

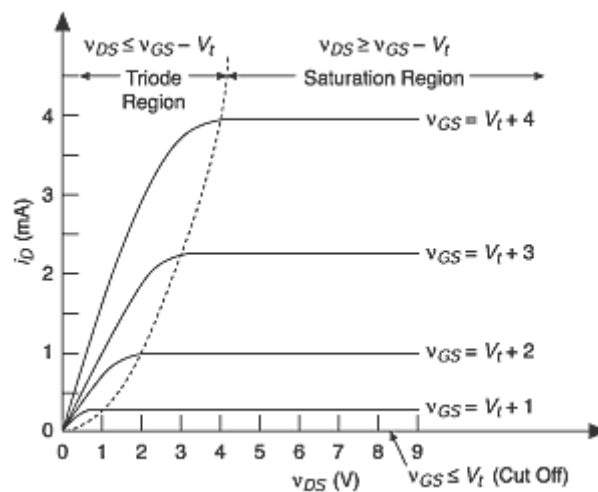


Figure 2.2  $I_D$  versus  $V_{GS}$  characteristics of MOSFET [21]

## 2.3 Importance of Scaling:

Scaling is a rev

Advantages of scaling include:

- It leads to smaller devices which ultimately leads to smaller chip area hence saving money.
- It also leads to reducing the gate delays which allow the possibility for higher frequency operation.
- Power dissipation is also reduced .

CMOS technology may be a promising technology to produce such a lot of benefits in device reducing to millimicron with the definite scaling.

## **2.4 Innovations in MOS Technology:**

### **2.4.1 Metal Gate**

To decrease the short channel effects and improve performance one way is to use metal gate. To further improve the device performance metal work function can be changed. Contacts can be either schottky or ohmic based on the work function difference.

### **2.4.2 Multi-Material Gate**

Multi-Gate material can be used to further increase the device performance. Moderately two or more (DMG) materials are used as material. As a result of this we can optimize electron speed and electric field. Multiple gates can be fused in accordance to the requirement to make schottky or ohmic contact[6].

### **2.4.3 Multiple Gates**

Multiple gate structure can be used to increase the performance. Because of multiple gate access to channel is easy which leads to better control over the drain current characteristics, also the leakage current can be reduced.

## **2.5 Limitations of MOSFET**

1) *Leakage current*- when  $V_{gs}$  is less than  $V_{th}$ , the drain current supposed to be zero but the current decreases exponentially. To measure this leakage current we take the help of sub threshold swing which is given by the amount of gate voltage applied to produce 10 times the change in current. Its value is constant to 60 mv/decade for leakage current to zero at room temperature. When scaling is done on the device to reduce power dissipation the sub threshold swing should be around 60 mv/decade. Leakage currents affect the current drastically since it affects power dissipation which ultimately affect the device operation in long time.

## 2) Short channel effects

a) *Velocity saturation effect* – Due to the scaling of MOSFETs to lower dimensions very high electric field is experienced by the charge carriers. Due to high electric field the velocity of carrier starts saturated which degrade the performance.

b) *Impact Ionization*- Due to high electric field the velocity of electrons is very high. They impact on silicon atoms which break the bond and create new electron and hole pair. This is called impact ionization.

c) *Hot carrier effect*- Due to this, the electrons and holes enter into dielectric after gaining high kinetic energy. This changes the capacitance of the system and makes it less reliable.

d) *Drain Induced Barrier Lowering* – In long channel length devices, the threshold voltage becomes independent of the drain voltage but in short channel device the drain voltage start influence the channel carrier which start flowing current at gate voltage less that threshold voltage.

## 2.6 FDSOI Transistor

### 2.6.1 Device Overview

Fully depleted silicon-on-insulator (FD-SOI), also called as ultra-thin or extremely thin silicon-on-insulator (ET-SOI), is thought of as an alternate to bulk element as a substrate for building CMOS devices. SOI wafers have a shallow layer of epitaxial element full-grown on top of suitable oxide layer that acts as an associate in used dielectric. The top silicon layer doesn't have any intrinsic charge carriers since it is fully depleted. This results in a number of advantages when building deep submicron devices.

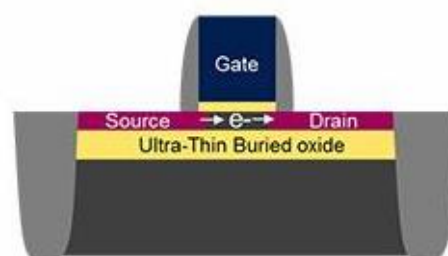


Fig 1.3 Structure of FDSOI[7]



## 2.6.2 Advantage and Disadvantage

### Advantage

1. FDSOI provides improved performance over the conventional bulk silicon made with micron processes, especially in circuits with low power. It has been seen that the current drive is lower in bulk devices also because of high insulating oxide under the channel it becomes difficult to turn off the device fully. In case of FD-SOI it is possible to keep the operating voltage lower by a value of 100-150 mV.
2. Reducing power supply in normal CMOS gives rise to noise margin which can lead to errors in memory array. With the help of FD-SOI it has been seen that the power consumption in power array has been reduced by a margin of forty per cent. This margin is achieved by only reducing the operating voltage.
3. Another potential favourable position of FD-SOI over the finFET, its closest rival for sub-28nm procedures, is that the methodology makes it conceivable to back-inclination the channel thus deal with the charge transporters coursing through it. The utilization of a slim channel manages different issues managed halfway exhausted SOI usage that utilized thicker silicon channels.
4. Biggest advantage of FD-SOI is that the channel can be back biased which means channel can be controlled from front or back. This enables us with better control over the channel and also the switching speed of device is improved. Even with scaling the effect of back-bias does not fades away while in case of bulk silicon it does. Back biasing effect has been used in proposed pH sensor. Effect at the threshold voltage gets amplified because of back-bias.
5. Even after the application of large reverse bias device does not leak much leakage current. This property becomes useful in case of low power applications.
6. In the FDSOI technology the desired threshold voltage is NOT set "by the defects on the interface between very shallow buried oxide and silicon". It is set by the polarity (n-type vs p-type) of the doping placed under the buried oxide.

## Disadvantage

The scaling on high scale of the device leads to very high OFF current and can vary the transistor performance. Also fabrication is tough for large scale production because source and drain are of different polarity and concentration than that of channel.

## 2.7 Literature Survey

T.Poiroux et al[9] wrote that Silicon film thickness has emerged as an important parameter which in turn determines the main electrical and transport properties of majority carriers in inversion layer. To make the film completely depleted from front interface to back interface it is needed that width of depletion region should be greater than silicon thickness. Coupling between front and back threshold voltage can be understood with the thickness between two interfaces. Method used to measure film thickness has an advantage that it does not need a strong bias voltage at the back gate like capacitive measurements.

Film thickness can be extracted using below formula[9]:

$$t_{si} = \frac{\epsilon_{si}}{\epsilon_{ox}} (t_{ox1} - \delta_2 t_{ox2}) \quad \text{equ(2.2)}$$

Where  $\delta_1$  and  $\delta_2$  are slope in the oxide and silicon region respectively and  $t_{ox2}$  is buried oxide thickness.

G. Tsutsui et al[10] wrote that effect of SOI thickness has been measured on  $V_{th}$ . As the thickness is brought down from 3 nm the  $V_{th}$  variation increases drastically. Threshold voltage variation can be considered as one of the critical issues in fully depleted silicon on insulator. Surface roughness contribution has also been calculated. Surface roughness of silicon on insulator interface fluctuates the body thickness which in result changes the SOI thickness.

To measure the effect of surface roughness following assumptions were made

1. Matching is done through the channel
2. At certain gate voltage, a thick to thin mash makes the inversion layer because of quantum confinement effect.
3. Randomness is provided independently for front and back interface.

Mobility variation induced  $V_{th}$  variation

Mobility is also affected by  $t_{SOI}$ . Mobility variation can be measured with the help of split CV method. S factor can be defined as[10]

$$S = \left( \frac{d(\log_{10} I_{DS})}{dV_{GS}} \right)^{-1} \quad \text{equ.}(2.3)$$

In simpler words threshold voltage variation can be induced by mobility variation SOI thickness, substrate bias and also because of quantum confinement effect.

*A general model to describe the electrostatic potential at electro light oxide interface[10]*

Several theories have been proposed by colloid chemist to describe how the charging mechanism occurs for metal oxides in electrolyte solutions. This in turn results into electrical double layer at oxide surface. Here another theory to describe electrostatic potential resulting at the metal oxide electrolyte solution interface was presented. Electrostatic potential variations were described as function of differential double layer capacitance and also the intrinsic buffer capacity.

Sensors work on the charging behavior of metal oxides in electrolyte solutions. This behavior has been studied using surface charge and zeta potential.in sensors like pH sensor variation in electrostatic potential has been used to determine the pH of electrolyte solution.

A direct relation was recognized between pH sensitivity and charging behavior of metal just after the introduction of ISFET. Site dissociation model has been used for a long time to describe the ISFET pH sensitivity given by its Yates. This in turn results into electrical double layer at oxide surface. Here another theory to describe electrostatic potential resulting at the metal oxide electrolyte solution interface was presented.

*General expression for the pH sensitivity of ISFET*

Bergveld and Sibbald gave the operational mechanism for the ISFETs using the following expression for drain current[10]:

$$I_D = \mu C_{ox} \frac{W}{L} \left( \left( V_{GS} - \left( (E_{ref} - \varphi_o + \gamma^{SOI} - \frac{\varphi_{Si}}{q} - \frac{Q_{ox} + Q_{SS}}{C_{ox}} \Big| \frac{Q_B}{C_{ox}} + 2\varphi_f \right) \right) V_{DS} - \frac{1}{2} V_{DS}^2 \right)$$

*equ.(2.4)*

Where  $\mu$  denotes the average electron mobility in the channel,  $w$  and  $l$  denotes the gate width and gate length,  $E_{ref}$  is the contribution of reference electrode,  $V_{gs}$  and  $V_{ds}$  our gate source voltage and drain source voltage respectively,  $\phi_{si}$  denotes silicon electron work function,  $C_{ox}$  denotes capacitance of gate oxide. Charge located in the oxide denoted by  $Q_{ox}$ , wild charge located in surface states and interface States denoted by  $Q_{ss}$  and  $Q_b$ .  $X_{soi}$  is surface dipole potential of the solution while  $\phi_f$  denotes the potential difference.

#### *The site dissociation model*

To describe the charging mechanism of double layer site dissociation model was developed. This model describes the charging of an oxide because of equilibrium between surface sites and  $h^+$  ions present in the solution. Equations derived show that hydrolysis of the surface shell create more surface sites which in result give rise in intrinsic buffer capacity and also the sensitivity.

Effect of silicon dioxide and aluminum oxide were also discussed.

#### *The Gouy-chapman Theory[10]*

This theory has been used to explain the capacitive behavior of electrolyte solution interface. Excess charge present in the solution side of interface can be considered equal in value as that of solid state surface but of opposite sign. Because of opposite sign ions present in the solutions are electrons statically attracted towards the solid-state surface. This attraction is counter acted by thermal motion which results in an equilibrium. This equilibrium between opposite trends can be understood with the help of well-known Boltzmann equation:

Y.-J. Huang et al [11]wrote that a double gate ion sensitive field effect transistor was studied having back side as sensing structure. It was implemented as high performance device with 180nm SoC platform. Bottom poly gate was used instead of fluidic gate to suppress non ideal effects such as time drift and hysteresis. This paper focuses mainly on improving the signal to noise ratio (SNR) along with sensitivity improvement. Sensitivity was improved to a maximum of 450mV along with SNR improved by 155 times. Also time drift reduced by 53 times. Sensitivity enhancement is considered 7.5 times higher over Nernst limit in usual DGFET.

pH sensitivity concept was used in the form of threshold voltage change when hydrogen ions that is  $H^+$  act with the sensing membrane. Double gate structure was used with open fluidic gate with the help of reference electrode and also one standard polysilicon gate. Simulations were done with both gate separately turned on one at a time and response were measured for both.

#### *Non-ideal Effect Reduction*

Liquid solution is considered as a bulk substrate. Here bottom poly gate was used for sensing. Important part about this work is that surface potential change amplifies the threshold voltage change for bottom gate because of capacitive coupling. In PG gate, time drift problem is greatly solved in contrast to single gate operation. Time drift is mainly caused because of solution charging and also because of large vertical electrical field. Successful time drift reduction was achieved from 5 hour to 10 minutes.

D. E. Yates et al[12]wrote that to explain interface charge at oxide electrolyte interface, a site bonding model was introduced. It was proposed that pairing occurs between absorbed counter ions and discrete charge surface groups. Surface charge density is an important parameter here. It can be measured using above model. Nernst equation had been used to relate the double layer potential to the activity in solution of  $H^+$  ions.

S. Koneshan et al[13] said that mobilities of various metal cations and anions like  $Li^+$ ,  $Na^+$ ,  $K^+$ ,  $F^-$ ,  $Cl^-$  etc. have been simulated here using molecular dynamics simulation with the help of SPC model for water. Mobilities of uncharged atoms were also simulated and found in agreement to Stokes' law. Mobilities are usually determined by solvent dynamics, structure, size and charge of the ions. Mobility in aqueous solution is also affected by water since it has hydrogen bonding and also affected by its network structure. These lead to abnormal behaviour in aqueous solution in contrast to computer simulations sometimes. Mobility, solvation structure and dynamics used here were not considered as dynamic variable but they usually are. Hydrodynamics as well as dielectric also lead to friction.

It was found that diffusion constant of uncharged Li is larger than of charged  $Li^+$  While the bigger iodine I is considered to have smaller diffusion constant than negatively charged  $I^-$ . This paper has been organized into six parts, 1<sup>st</sup> one includes

simulation for diffusion constants of charged and charged solutes while 2<sup>nd</sup> parts includes description about solvation dynamics of cation and anions. Part three describe about residence times of water in shells surrounding the ions while part describe about the structure of these shells.

H. J. Jang et al [14]wrote that Fully Depleted SOI (FDSOI) fabrication has been done here containing double gate structure. It was observed that for single gate operation pH sensitivity remains lower than Nernstian limit at 47.9mV/pH. While the double gate performance has been measured at 379.2 mV/pH which is significantly higher than the Nernstian limit. Standard MOSFET has been modified by replacing glass electrode with electrolyte and reference electrode. Since interactions occur at interface of glass electrode and electrolyte which leads to variation in surface potential .Since biological sensor can operate in equilibrium condition, it comes as an advantage. Simulations have been done by varying the gate dielectric byAl<sub>2</sub>O<sub>3</sub>, Er<sub>2</sub>O<sub>3</sub>, Ta<sub>2</sub>O<sub>5</sub> but still poor sensitivity was obtained with these membranes.

In normal cases a reference electrode is used at the top of sensing membrane where electrolyte is put. This allows electrostatic coupling with the channel. In this paper Double gate structure has been used in contrast to single gate structure This also helps in improving signal to noise ratio.

Fabrication steps have been defined along with simulation results with front and back gate sweep. Back gate requires more gate voltage than front gate sweep but sensitivity is achieved more in back gate seep rather than front gate sweep.

During simulation non ideal effects such as hysteresis width and drift rate also affect device operation. Electrolyte solution can also penetrate the sensing membrane which can affect effective oxide thickness. Because of change in oxide thickness gate capacitance also changes. This deterioration of sensing membrane can be controlled by using high k oxide material. Although effect of these non-ideal effects is less in single gate operations but sensitivity improvement is much more in double gate operation.

Ajay et al[18] wrote that device has been simulated as pH sensor within Nernst limit having sensitivity less than 60mV. Analytical modeling has been done for junctionless device. Other than that simulation methodology has been explained. Electrolyte has been simulated by changing the mobility with Na<sup>+</sup> and Cl<sup>-</sup> ions mobilities. pH change

has been defined by change in density of states since Poisson Boltzmann equation is very similar to semiconductor equation[17]. Simulation has been done for various oxides such  $\text{SiO}_2$ ,  $\text{Si}_3\text{N}_4$ ,  $\text{Al}_2\text{O}_3$ ,  $\text{HfO}_2$  and  $\text{Ta}_2\text{O}_5$ . Sensitivity has been simulated for all five oxides. All five oxides show similar behavior except characteristics are shifted left or right but device still lacks in most basic area which is sensitivity. Junctionless channel gives advantage like easy fabrication and lower leakage currents.

Above papers have been briefly surveyed and gaps have been discussed. Also the required concepts and history has been discussed which might be helpful during this project. Earlier discussed papers had gaps regarding higher sensitivity. These gaps might be covered with the help of suitable oxide and channel material. For better results, approach is to use different oxides along with different channel material. Oxides decide to use are  $\text{SiO}_2$ ,  $\text{Si}_3\text{N}_4$ ,  $\text{Al}_2\text{O}_3$  which can be used with Silicon and SiGe. Sensitivity will be discussed along with effect on channel potential and device performance will be discussed. pH sensitivity will be discussed over a wide range of simulations and results will be drawn. Device performance will be discussed after unity gain frequency analysis.

---

### 3.1: Introduction

Atlas software provides simulation based general solutions for based on physical simulation may it be two or three-dimensional (2D,3D) simulation. Atlas tool is made in such a way such that tool may be used along with the VWF based Interactive Tools. These VWF tools are also known as Virtual Wafer based Fabrication Interactive Tools. These are made of the following: Tony Plot, Optimizer, MaskViews, Deck Build and also DevEdit[15].

Function can be explained as below:

- Deck Build is a window which is used for all command instructions.
- Devedit makes it possible to craft structure of device and also helps in designing the meshes which is used in a very cooperative surrounding.
- Optimizer can be used across various simulators to provide Optimization.
- MaskViews help in providing IC layout correction.
- TonyPlot is like the output window which is used to actually display the various electrical characteristics such as drain current for the device as well as also display the generated structure files. These files can be reopened with the help of TonyPlot.

Since the results of VWF Tools simulation based results are closely similar with new advancement in technology and hence results obtained are very similar to experimentation done. These tools can be very useful since they are very similar to approaching technology. It has also proved to be helpful in prediction of nearly all the current and voltage related characteristics and options related to the all new devices and also processes of technology.

Similar to Atlas, one other process simulator, is named as Athena. This can also produce prepared structures through many process based steps. It is mainly used in fabrication related devices. The same structure can be used by Atlas in form of inputs. Later various electrical characteristics can be predicted about the designed device with the help of Atlas. Next stage include providing the output of the Atlas to the SPICE modelling code and produce device based characterization at last.



Atlas can also be considered as simulation machine based on physical simulations for devices because this is capable of finding characteristics like drain current, frequency analysis etc. related to a specific device with selected structure and also the voltage outputs present at the electrodes. Simulators make the complete device space with grid like structure known as meshes and end known as nodes. Differential equations based Maxwell's laws and current conduction are applied at every location throughout the structure which helps in determining the electrical parameters. Being physically based device simulator has several advantages because without fabricating the device directly, a deep understanding can be brought about the device. Calculation of many complex parameters becomes easy and quick. It also helps in approximation of the output ,also the input can be varied in stepwise manner to get very close discrete output.

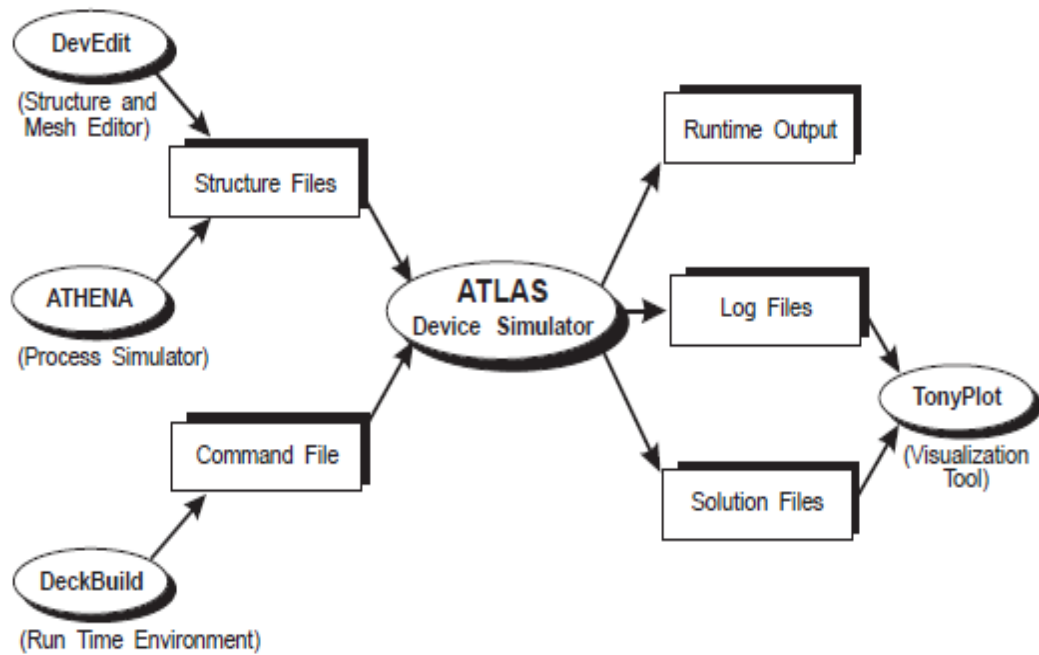


Figure.3.1: Atlas device simulator[15].

Above diagram explains how the information flow through Atlas device simulation (Figure3.1).Code is written on the text file which is run through the atlas simulator which in result is saved into a structure and log file.

Atlas mainly has three types of output files:

- Runtime output provides necessary data to be processed at every execution of atlas commands. It also shows errors and warnings at the same time.
- Log file data can be run later through tonyplot tool to plot required graphs.

- Log files also provide all necessary electrical characteristics like drain current, trans conductance etc.

### 3.2: Step for Defining the Structure

Required ATLAS Commands for defining the structure:

A specific commands set must be used to define a structure via SILVACO tool[15].

These commands can be used as listed below.

The first step includes the definition of the mesh specification.

#### Step 1. Define Meshing:

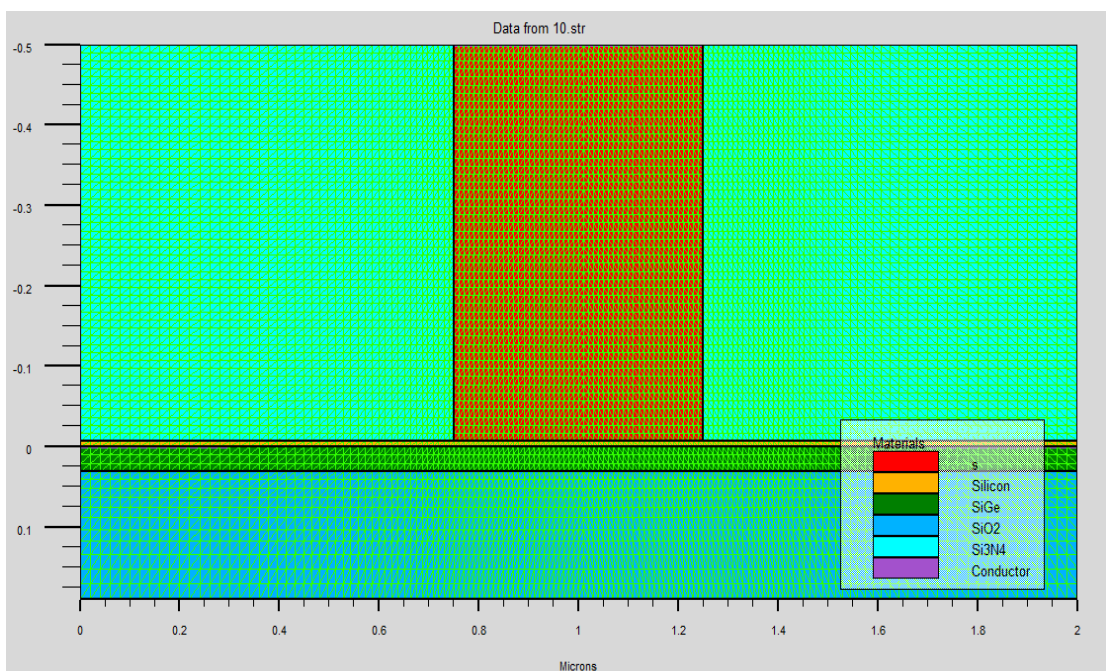


Fig 3.2 Meshing in the Structure

Mesh.mult statement can be used to multiply the spacing between meshes. Spacing will be changed by provided factor. Meshes can be made finer or denser as needed.

Syntax:

*MESH SPACE.MULT*=<value>

Now we need to define the horizontal and vertical meshing using x.mesh and also y.mesh.

*X.MESH LOC*=<value2>*SPAC* =<value1>

*Y.MESH LOC*=<value4>*SPAC*=<value3>

here *value2* and *value4* can be used to specify the position of horizontal and vertical mesh line each in microns and *value1* and *value3* defines the gap in between each mesh lines.

Then in next step we need to divide the structure into various regions. These various regions might be made of various different materials along with a very specific doping profile. Following commands can be used to specify the region.

### Step 2.Region Definition:

```
REGIONNUMBER=<value>X.MIN=<value5>X.MAX=<value6>Y.MIN<value7>Y.
MAX=<value8>MATERIAL=<material9>
```

The region number may be given by code word *value* and *value5* to *value6* provides the range on needed the x-axis while *value7* to *value8* provide range on respective y-axis. *Material9* defines the material used such as SiO<sub>2</sub>

```
region num=1 user.material=s x.min=0.75 x.max=1.25 y.min=-0.5 y.max=-0.005
```

Above line defines the region location used for dielectric.

```
material material=s user.group=Semiconductor user.default=Si mun=6.88e-4
mup=4.98e-4 nc300=2.333e26 nv300=2.33e26 eg300=1.5 permittivity=78
affinity=3.9
```

Electrolyte can be replaced with intrinsic semiconductor which will mimic like electrolyte solution with mobility and density of states replaced along with permittivity.

```
region num=5 material=nitride x.min=0 x.max=0.75 y.min=-0.5 y.max=-0.008
```

```
region num=6 material=nitride x.min=1.25 x.max=2 y.min=-0.5 y.max=-0.008
```

Area surrounding the electrolyte can replaced with dielectric such as silicon nitride using above instructions. This area can also be replaced with air as dielectric. This is required to perform successful meshing.

### Step 3. Define Electrode:

ELECTRODENAME<*electrodename*>NUMBER=<*value1*>X.MIN=<*value2*>X.M  
AX=<*value3*>Y.MIN<  
*Value4*>Y.MAX=<*value5*>

Where electrode name is given as *electrodename*. Electrode location is from y.min to y.max and x.min to x.max.

electrode name=gate1 x.min=0.75 x.max=1.25 y.min=-0.5 y.max=-0.5

Doping region can be used with following syntax which is

DOPING<*type of profile*>CONC =<*value*><*type of doping*>REGION=<*number3*>

Doping type can be set by *type of doping* and value can be changed by *value*.

The doping profile is mostly uniform but sometimes Gaussian.

*doping uniform conc=1e17 reg=3 p.type*

*doping gauss n.type conc=1e20 char=0.2 lat.char=0.05 reg=3 x.r=0.7*

*doping gauss n.type conc=1e20 char=0.2 lat.char=0.05 reg=3 x.l=1.3*

Channel under the gate is having p-type doping with  $10^{17}$ cm<sup>-3</sup> concentration while remaining region is having n-type doping with  $10^{20}$ cm<sup>-3</sup> concentration with Gaussian distribution.

### Step 4. Contact Definition:

Contacts can be defined using following syntax:

CONTACT NAME<*name of contact*>WORKFUNCTION=<*value2*>

where *name of contact* will set the contact name whereas *value* will specify about its work function.

Contacts can also be defined by directly using defined contacts like N.Polysilicon, Tungsten, Aluminium, P.Polysilicon etc. These have already defined work functions.

These contacts can be used with following command:

*CONTACT NAME<b.gate> N.Polysilicon.*

Some times we might need to define external inductors, resistors and capacitors.

Following syntax can be used for that.

*CONTACT NAME=<name of contact> RESISTANCE=<value3>*

*CAPACITANCE=<value4> INDUCTANCE=<value5>*

Here value3, value4 and value5 can be used to specify the values of resistance(ohm), capacitance(Farad), inductance(Henry) respectively.

### 3.3: Specification of Models

MODELS statement is required mainly to define the way device is simulating. These include physical models usually required in simulations. This does not include impact ionization but can be used by writing IMPACT statement. Whatever phenomenon occurs inside the device will affect the choice of models. Mainly models can be categorized into five parts[15].

- a. Mobility Model
- b. Impact Ionization Model
- c. Recombination Model
- d. Carrier Statistics Model
- e. Tunnelling and Carrier Injection Model.

### 3.4: Commonly Used Models

#### 1. *Concentration-Dependent Low-Field Mobility Model:*

CONMOB command can be used for activation of this model. This model provides all the necessary required data needed for low field based mobility for holes as well as electrons.

#### 2. *Analytic Low Field Mobility Model:*

ANALYTIC command is to be used in the MODEL statement. This model will help in specifying doping dependent low field mobility and temperature. Silicon is by default defined for this model at 300K.

#### 3. *Shockley-Read-Hall Recombination Model:*

The SRH parameter can be used in the MODELS statement to activate this model. There are a few user-definable parameters like TAUN0 and TAUP0 can be used in the MATERIAL statement that denotes the electron and hole lifetime parameters. This model indicates the recombination of electron and hole through Shockley-Read-Hall recombination.

#### 4. Auger Recombination Model:

AUGER statement is to be used to activate this model. The coefficients for holes and electrons for this model can be defined by user as needed. The coefficients like  $aug_n$  and  $aug_p$ , can be included in the MATERIAL statement.

## 5. Fermi-Dirac Model

This model follows the idea of Fermi-Dirac statistics. It is mainly used in the regions which are heavily doped but having reduced concentrations for the carrier. FERMI command is to be used to activate in the MODELS statement.

### 3.5: Numerical Methods

The numerical methods statements are specified under the METHODS statement. Three types of techniques are there to find solution[15].

1. Gummel
2. Newton
3. Block

The first method can be used to find the solution for one unknown variable when the rest of the variables are constant. This method will continue calculating till a stable resolution has been obtained. Unlike the previous gummel method, 2<sup>nd</sup> method newton method will solve and find all the unknown parameter at the same time. Block method is in between gummel and newton strategies since it will solve a few unknown at a time.

### 3.6: Methods to Obtain Solutions

All parameters such as current, transconductance, electric field and also capacitance can be calculated, we just need to apply voltages at electrodes such as drain and source. Gate biasing is to be done also. First, we start with zero bias but after that biasing can be varied in either direction in form of small steps. All these things need to be included in SOLVE statement.

#### 1. DC Solution

Fixed DC bias can be applied on the any required electrode with the help of DC solve statement.

SOLVE <v.name of electrode>=<value>.

According to the statement *name of electrode* the required electrode, can be supplied with value of DC voltage.

Following command can be used to sweep voltage from *value3* to *value5* in steps of *step4*. Electrode name can be specified with *name of electrode* statement.

SOLVE <v.electrode name>=<value3> VSTEP=<step4> VFINAL=<value5>

## 2. AC Solution

AC solutions can also be obtained similar to DC solutions. Similar command is to be used. AC simulation is necessary to find capacitance and conductance between any pair of electrodes. We just need to perform a post processing operation to DC solutions. The command used for this is

```
SOLVE VBASE=0.7 AC FREQ=1e9 FSTEP=1e9 NFSTEPS=10
```

### 3.7: Prediction of Results

There are three types of output files in Atlas [15].

They are:

#### 1. Log Files

Log files are used for recording current and voltage characteristics simulated by Atlas. It includes voltages and current of each electrode included during the simulations. Time is varying parameter during transient analysis. In case of AC analysis, capacitance and transconductance is saved.

#### 2. Run-Time Output

It is the window at the bottom of deckbuild. It will display any errors occurred during the simulations. This also displays every running command at that instant.

#### 3. Extraction of parameters In Deck Build

For extraction of various parameters command used is EXTRACT. This command helps in extraction of parameters like drain current etc. This can be used to extract from earlier solved structure or log file. The command includes a versatile syntax that permits you to construct specific EXTRACT routines.

---

#### 4.1: Different Types of SOI MOSFETS:

##### **Planar Bulk:**

In Planar bulk devices, electrons will move from source to drain through the bulk. Because of this there can be leakage into the bulk which will in turn affect power consumption and device performance. The Silicon on Insulator wafer is formed by depositing a thick buried oxide (BOX) layer on top of the bulk silicon wafer. After that an epitaxial silicon layer is deposited on top of the oxide. On the top silicon layer Transistors are formed, and are isolated from the substrate by the oxide layer.

##### **Partially Depleted SOI (PDSOI):**

PDSOI or Partially Depleted SOI MOSFETs are the successors of earlier SOS (Silicon – on - Sapphire) devices. As suggested by the name body is partially depleted and remains independent from bulk substrate. Floating body improves the performance but also introduces some peculiarities. In this, a small neutral region can be deposited under gate in the depletion region. Here, channel thickness is more than that in FDSOI. This is known as partially depleted SOI (PDSOI). However, PDSOI tends to have higher  $V_T$  which leads to slower operation and larger gate-effects as compared to FDSOI which leads to larger leakage currents. Hence, FDSOI is mainly used for small process nodes (below 90nm).

##### **Fully Depleted SOI (FDSOI):**

In this technique, the MOS placed over an ultra-thin oxide film which insulates the cell from rest of the body. A very thin layer of silicon is deposited on top of this oxide film which acts as a channel. Since the channel is very thin, channel can be established in this layer without any more additional doping of the same. Because of this reason, it is known as fully depleted SOI. This technique has various advantages like reduced components of leakage currents like  $GIDL$ , gate tunneling currents etc. which are dominant in lower technology nodes. Fully Depleted SOI devices have a better electrostatic coupling between the gate and the channel. This technology has advantages like better linearity, sub-threshold slope, body coefficient and current



drive. FDSOI technology has found applications in a number of applications ranging from low voltage, low-power to RF integrated circuits.

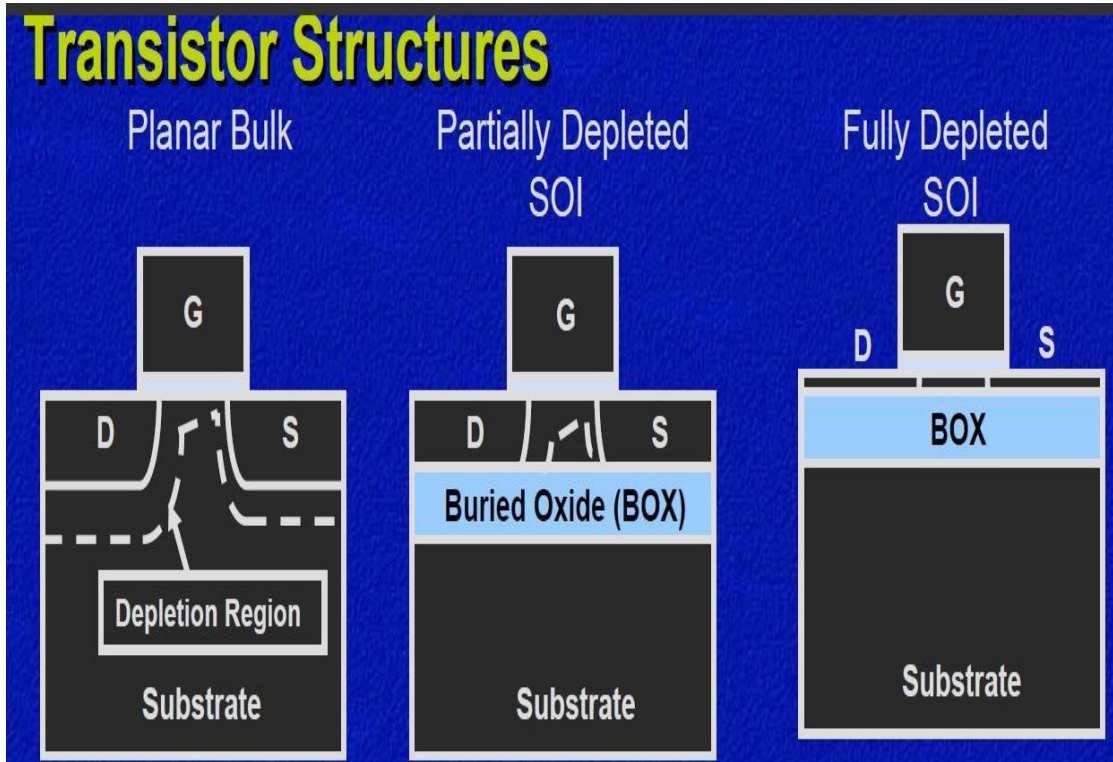


Fig. 4.1 different types of SOI MOSFET structures [16]

#### 4.2: Device Structure

The cross-sectional view of the FD SOI -based pH sensor is shown in Fig4.2. From Fig. 4.2, it is clear that in the case of pH-FD SOI design, the channel region has the  $10^{17}\text{cm}^{-3}$  p-type doping concentration rather than  $10^{20}\text{cm}^{-3}$  in the source and drain regions. The channel length (L) is 500 nm. Electrolyte has been covered from both side by oxide taken as nitride. Channel width is taken as 30nm and oxide is taken at 7nm. BOX width is kept at 160nm. These dimensions have been optimized for better results in leakage current and sensitivity results. Doping concentration have been simulated so that to get better results. Electrolyte has been simulated with 500 nm length tken as an intrinsic semiconductor but it has been optimized to act like an electrolyte by changing the mobility and relative permittivity.

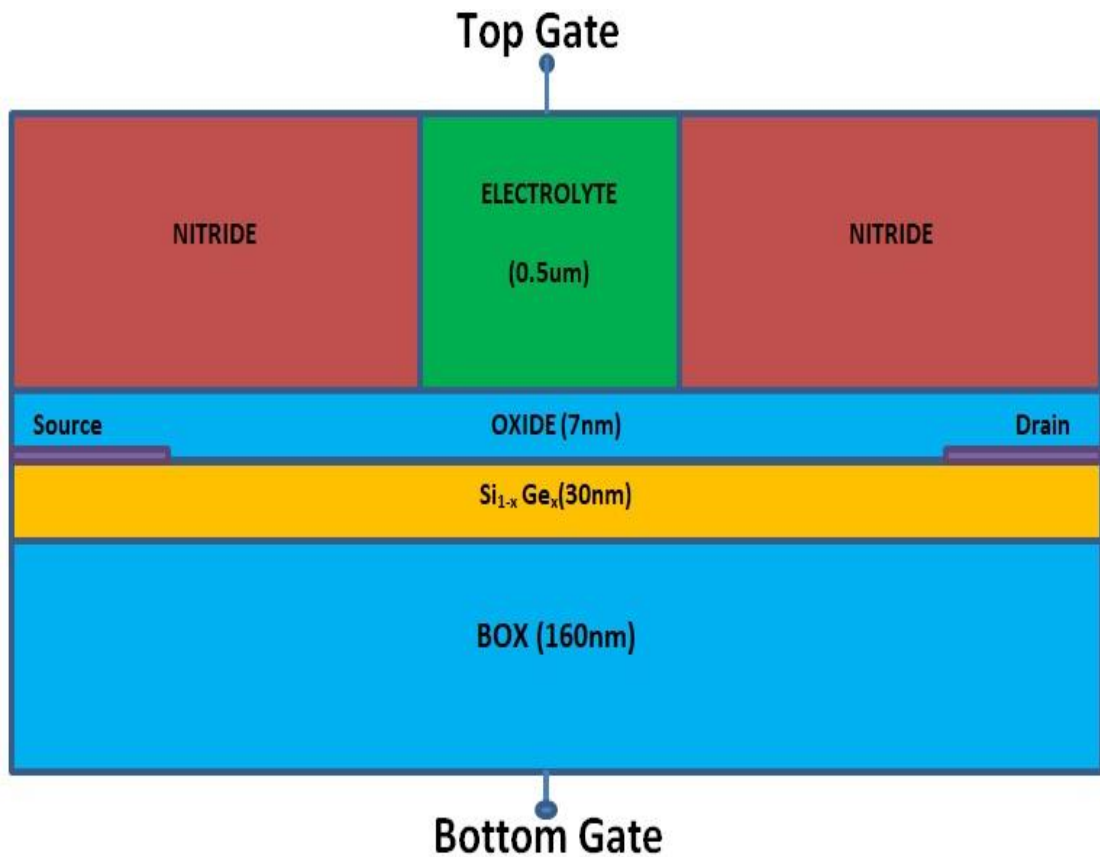


Fig.4.2 Device Structure

In real ionic solution the Poisson-Boltzmann equation can be used to define the charge distribution. This equation (PB equation) is very close to the semiconductor equation, but there are some differences with Fermi-Dirac distribution of charges of electrons and holes in the semiconductor[19]. With the changed mobility of electrons and holes of the intrinsic semiconductor the simulation has been performed for the salt concentration. The mobility of the holes and electrons has been changed in the salt concentration due to the  $\text{Cl}^-$  and  $\text{Na}^+$  ions, the electron mobility has been replaced by the  $\text{Cl}^-$  ions in water with the value of  $6.99 \times 10^{-4} \text{ cm}^2 \text{ V}^{-1} \text{ S}^{-1}$  and mobility of holes is now the mobility of  $\text{Na}^+$  ions mobility valued  $4.98 \times 10^{-4} \text{ cm}^2 \text{ V}^{-1} \text{ S}^{-1}$ [19]. The above mentioned mobility values have been calculated using the Einstein equation  $\mu = D/kT$ , where T denotes absolute temperature and k denotes boltzmann constant and D denotes Diffusion constant. These substitution have been done so that the solution will mimic like a pH solution. These substitutions have been confirmed by earlier simulations. Further these pH values will be changed with the help of change in density of states.

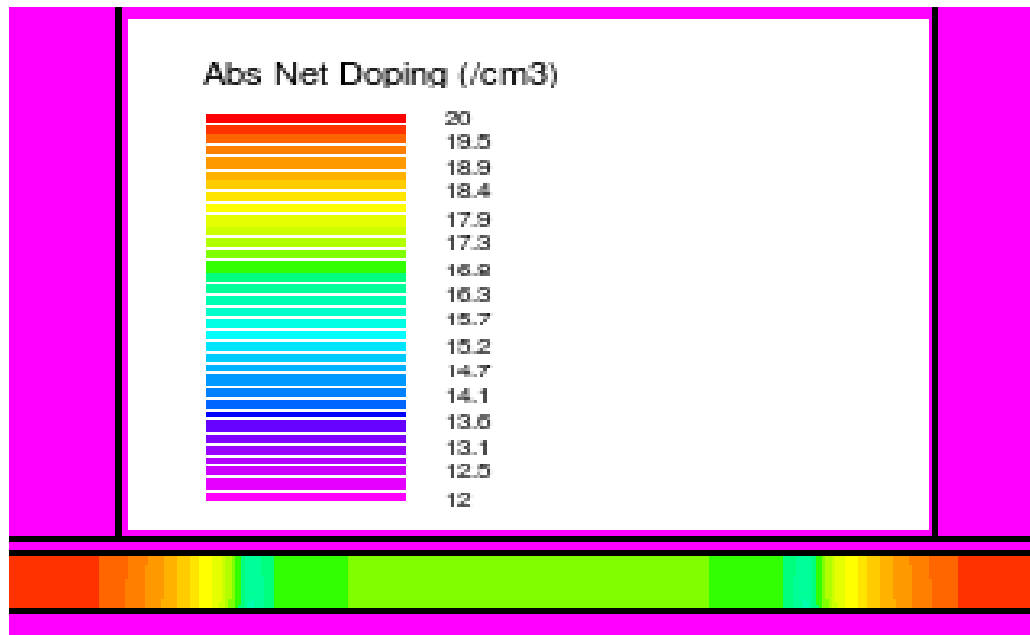


Fig.4.3 Channel doping

Values of different Oxides:

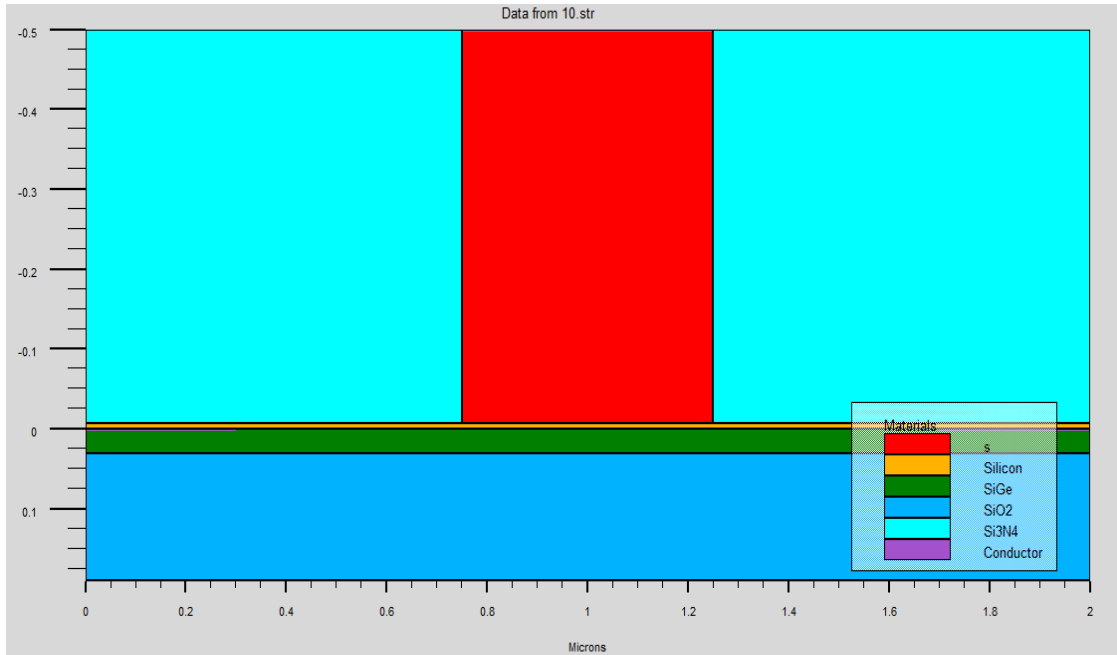
Gate Oxide	Relative Permittivity	Ns(cm <sup>-2</sup> )	Ref.
SiO <sub>2</sub>	3.9	5*10 <sup>14</sup>	[18]
Si <sub>3</sub> N <sub>4</sub>	7.5	3*10 <sup>14</sup>	[18]
Al <sub>2</sub> O <sub>3</sub>	14	8*10 <sup>14</sup>	[18]

Table 4.1

Device Dimensions:

Parameter Name	Parameter Value	Parameter Name	Parameter Value
Channel Length	500 nm	Channel Doping	5*10 <sup>17</sup> (p-type)
Channel Thickness	30	Source/Drain Doping	5*10 <sup>20</sup> (n-type)
Channel Width	1 μm	BOX Thickness	160 nm
Oxide Thickness	7 nm		

Table 4.2



*Fig 4.4 Simulated Structure*

### 4.3 Device Operation

Density of states in semiconductor in the valence and conduction bands,  $N_v$  and  $N_c$  are considered as most important parameters for correlation in between the electrical characteristics for an intrinsic semiconductor and physical properties for the solution. Holes and electrons can act like mobile ions corresponding to electrolyte solution. Molar concentration for aqueous solution can be defined with the help of density of states  $N_v$  and  $N_c$ . Dissociation of  $H_2O$  occurs into  $H^+$  and  $OH^-$  under equilibrium, hence mass action law can be defined as ions product of water is defined by[19]

$$K_w = [H^+] [OH^-]$$

Since we know In pure water at 25 °C

$$\begin{aligned} [H^+] &= [OH^-] = 1 \times 10^{-7} \text{ mol/L} \\ K_w &= (1.0 \times 10^{-7} \text{ mol/L})(1.0 \times 10^{-7} \text{ mol/L}) \\ &= 1.0 \times 10^{-14} \text{ mol}^2/\text{L}^2. \end{aligned}$$

The mass action law for water is considered to be very similar to the mass action law in the case of intrinsic semiconductor. The mass action law states that under thermal equilibrium, of the product the free electron  $n$  and the free hole concentration  $p$  and is equal to the square of the intrinsic carrier concentration  $n_i$ . The carrier concentration can be approximated with the help of the Boltzmann statistics, which is given as[21]

$$p = N_v e^{-\frac{E_f - E_v}{kT}} \quad \text{equ.(4.1)}$$

$$n = N_c e^{-\frac{E_c - E_f}{kT}} \quad \text{equ.(4.2)}$$

where  $E_v$  is the upper energy level of the valence band,  $E_c$  is the lower value level of the conduction band,  $E_f$  is the Fermi level, and  $k$  is the Boltzmann constant.

$$np = N_c N_v e^{-\frac{E_G}{kT}} = n_i^2 \quad \text{equ.(4.3)}$$

$$N_c = 2 \left[ \frac{2\pi m_e^* kT}{h^2} \right]^{\frac{3}{2}} \quad N_v = 2 \left[ \frac{2\pi m_h^* kT}{h^2} \right]^{\frac{3}{2}} \quad \text{equ.(4.4)}$$

where  $m_h$  and  $m_e$  represent their effective mass of holes and electrons for their density of state calculations and  $h$  denotes Planck's constant[21]. For the calculation of the electrolyte equivalent semiconductor  $N_c$  and  $N_v$  value, the Avogadro constant  $N_A = 6.022 \times 10^{23} \text{ mol}^{-1}$  can be converted into  $1 \text{ mol/L} = 6.022 \times 10^{23}/\text{L} = 6.022 \times 10^{20} \text{ cm}^{-3}$  and it can be assumed that  $[\text{H}^+] = p$  and  $[\text{OH}^-] = n$ . Hence, solution with a  $\text{pH} = 7$ , the ion concentration for  $[\text{H}^+] = 10^{-7} \text{ mol/L}$ , which relates for the hole concentration  $p = 10^{-7} \times 6.022 \times 10^{20} / \text{cm}^3 = 6.022 \times 10^{13} / \text{cm}^3$ .

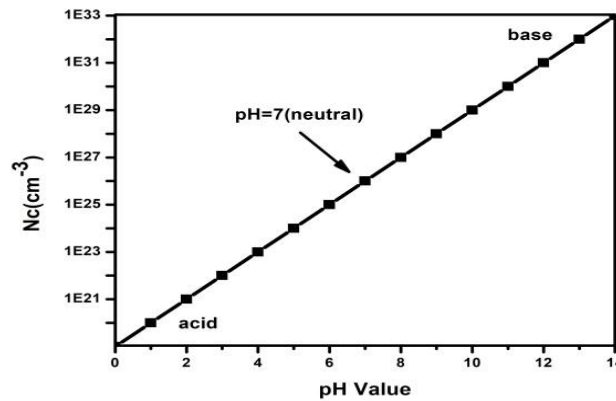


Fig. 4.5. Variation of density of states of conduction band with respect to pH value

By putting this value in (4.4), the equivalent density of states corresponding to the valence band may be found as  $N_v = 2.33 \times 10^{26} \text{ cm}^{-3}$  by taking  $E_g = 1.5 \text{ eV}$ . A similar procedure may be used to find out the density of states for the conduction band, i.e.,  $N_c$ . For  $\text{pH} = 7$ , the concentration for the ion  $[\text{OH}^-] = [\text{H}^+]$ ; hence,  $N_c = 2.33 \times 10^{26} \text{ cm}^{-3}$ . For  $\text{pH} = 9$ ,  $[\text{H}^+] = 10^{-9} \text{ mol/L}$ , and  $[\text{OH}^-] = 10^{-5} \text{ mol/L}$ , the corresponding value

of  $N_V = 2.33 \times 10^{28} \text{ cm}^{-3}$  and  $N_C = 2.33 \times 10^{24} \text{ cm}^{-3}$ . For  $\text{pH} = 4$ ,  $[\text{H}^+] = 10^{-4} \text{ mol/L}$ , and  $[\text{OH}^-] = 10^{-10} \text{ mol/L}$ , the corresponding value of  $N_V = 2.33 \times 10^{23} \text{ cm}^{-3}$  and  $N_C = 2.33 \times 10^{29} \text{ cm}^{-7}$ . The ionic charge concentration in the electrolyte, which is given as[21]

$$n_0 = N_V = N_C = N_{\text{avo}} i_0 \times 10^{-3} \quad \text{equ.(4.5)}$$

where  $N_{\text{avo}}$  denotes Avogadro's number (1/mol) and  $i_0$  denotes the ion molar concentration ( $1\text{M} = 1000 \text{ mol/m}^3$ ) present in the solution bulk and  $n_0$  denotes the ionic charge based concentration for the electrolyte, which can be considered equal to the density of state of intrinsic semiconductor material.

#### 4.4 Classification of Sensor

*First Class Of The Sensor:*

*Active Sensors:* These sensors come under the category which always require an external source excitation signal or a external power signal. Without power these are useless. E.g. : temperature sensors, gyro sensor, alcohol sensor etc .

*Passive Sensors:* These sensors do not usually require any kind of external power signal and hence can directly generate required output response. Eg : infrared based camera. They capture images using heat energy.

*Second Class Of The Sensor:*

This class is dependent on the method of detection. Some of the methods of detection are Electric, pH sensor, Radioactive sensor, Biological sensor, Chemical sensor etc.

*Third Class Of The Sensor\_:*

This class follows the conversion phenomenon i.e.it covertes the input data from one form to another form. Some of the various common conversion phenomena based sensors include Photoelectric (conversion from light into energy), Thermoelectric (heat into electricity), Electrochemical, Electromagnetic, Thermo optic, etc.

*Fourth Class Of The Sensor\_:*

This class contains digital and analog sensors. Analog output is generated by analog sensors which generates output signal with continuous stream of quantity under measurement. Digital sensors store the measured data in form of discrete values. These values can be stored in a file and compared at later date.

#### **4.5 Types of Sensor in Electronics**

Sensors can be used for measuring any one of the physical properties like Heat Transfer, Temperature, Resistance, Conduction, Capacitance, etc. are often used in most of the electronics applications.

1. Accelerometer
2. Temperature Sensor
3. IR Sensor (Infrared Sensor)
4. Smoke, Gas and Alcohol Sensor
5. Touch Sensor
6. Ultrasonic Sensor
7. Proximity Sensor
8. Light Sensor
9. Pressure Sensor

$I_D$  and  $g_m$  are the sensing performance metrics that needs to be focused during the design of a sensor. Here, the performance analysis of Si based FD-SOI has been compared with proposed SiGe based device. The advantage of using  $Al_2O_3$  as gate dielectric has also been presented through sensitivity analysis for pH detection. For making feasible the pH detection using simulations, the electrolytic region has been defined as an intrinsic semiconductor whose density of states are varied with respect to the pH of the electrolytic solution of interest.

### 5.1 Impact of pH Immobilization on Device Threshold Voltage:

Threshold voltage can be used as sensing metric to analyze and optimize the device sensitivity. Here 3 different dielectric based FD-SOI's have been simulated and investigation has been done on the variation in threshold voltage with pH immobilization.

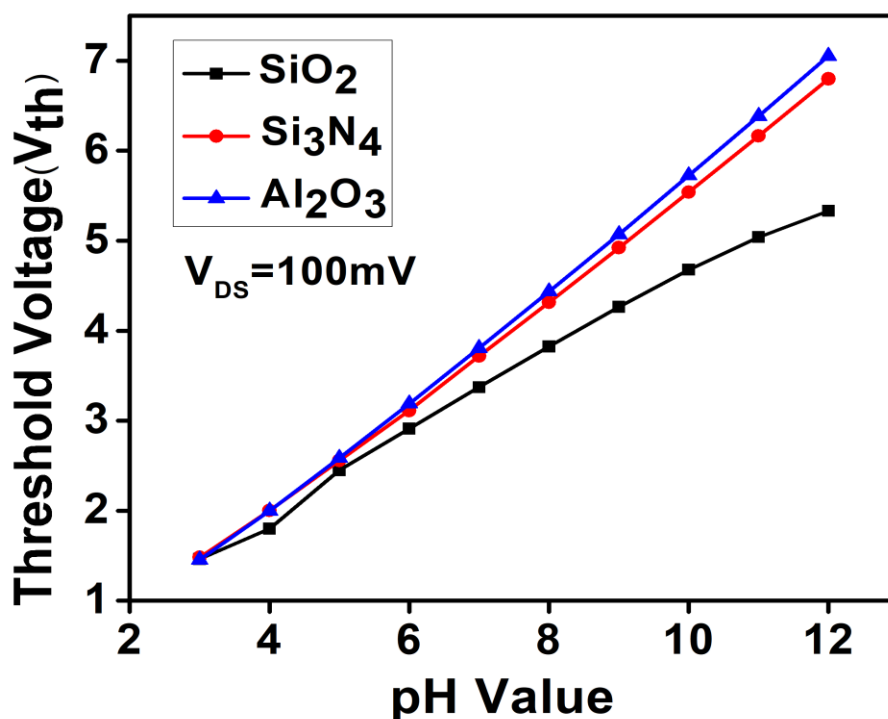


Fig 5.1 Threshold voltage shift with pH immobilization



It has been observed that Al<sub>2</sub>O<sub>3</sub> based FD-SOI outperforms the Si<sub>3</sub>N<sub>4</sub> and SiO<sub>2</sub> based systems as shown in Fig.5.1. When the pH of the electrolyte increases the threshold voltage is found to increase. All the devices simulated gives good resolution, the average sensitivity of SiO<sub>2</sub> based device is found to be 450mV/pH (when pH is increased from 7 to 8) which increases to 597mV/pH when SiO<sub>2</sub> gets replaced by Si<sub>3</sub>N<sub>4</sub> and further to 629mV/pH when Al<sub>2</sub>O<sub>3</sub> is used. Further the substrate material has been changed from Si to SiGe and sensitivity analysis has been done. As Al<sub>2</sub>O<sub>3</sub> gives the best performance among the other dielectric counterparts here simulation has been done only with this single dielectric. The advantage of using SiGe over Si is that, the high mobility of electrons in Ge can help in yielding higher device sensitivities. The SiGe based device showcases 13.18% (when Al<sub>2</sub>O<sub>3</sub> is used as gate dielectric in both devices under comparison) increased V<sub>th</sub> based sensitivity were the V<sub>th</sub> shifts by 712mV when pH of the electrolyte is increased from 7 to 8. The overall device sensitivity of the device can be evaluated using the equation. Effect of high k material is also observed in relation to electrolyte solution. High k oxide is not easily penetrated by electrolyte during real time usage. This helps in long term practical usage[19].

$$\Delta V_{th} \text{ sensitivity} = \left| \frac{V_{th1} - V_{th2}}{pH_1 - pH_2} \right| \quad \text{equ.(5.1)}$$

## 5.2 pH sensing performance for various oxides:

Channel material is kept same as silicon for these simulations, Whereas the oxide will be changed with SiO<sub>2</sub>, Si<sub>3</sub>N<sub>4</sub> and Al<sub>2</sub>O<sub>3</sub> respectively. Performance comparison will be done in form of threshold voltage shifts for various pH. Drain current shifts to the right as value of the pH increases. Oxide selection may help in many aspects such high sensitivity and longer device life time. Since electrolyte contact might affect device working because electrolyte being acidic might degrade the oxide which will affect the site binding charge and in turn affect device performance. Oxide selection might also affect in terms of power consumption. Some oxides might results in better sensitivity but poor in power saving. High leakage current might lead to power drainage. Selection must be made on the base of requirement whether we want high sensitivity or power saving is more important.

### 5.2.1 SiO<sub>2</sub> as Oxide:

With SiO<sub>2</sub> as oxide, Drain Current versus Gate bias voltage is drawn. SiO<sub>2</sub> has been used as an oxide for a long time for its easy availability. As the pH value is increased in the form change in the density of states, Drain current sees a shift in the Drain current. Change is also observed in the form of threshold voltage. Simulation has been performed at 100mV of drain to source voltage. Results have been plotted in logarithmic y axis. Results show much better shift than previous results discussed in literature review. Most of the devices have been limited to Nernst limit. Being double gate helps it to surpass that limit. This change in threshold voltage is proportional to sensitivity. Graph shifts to right as the solution changes from acidic to basic. Maximum threshold shift has been observed as 450mV for SiO<sub>2</sub>.

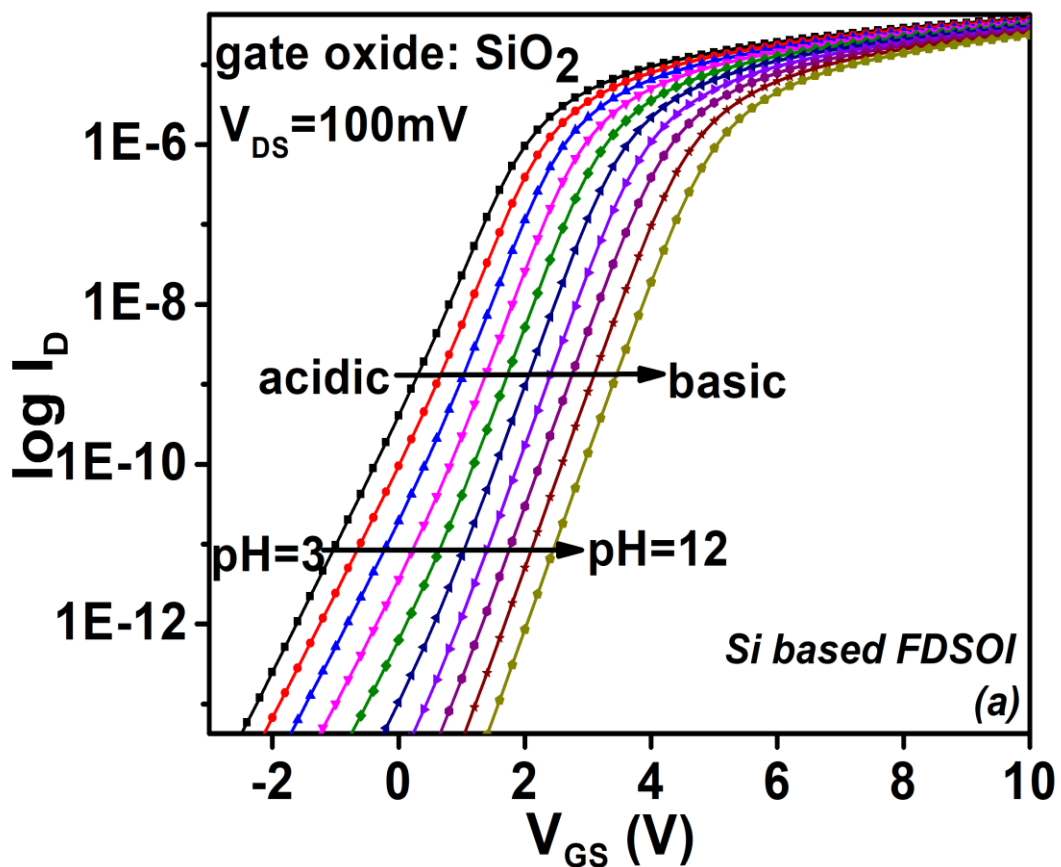


Fig 5.2 pH Sensing characteristics for SiO<sub>2</sub>

### 5.2.2 Si<sub>3</sub>N<sub>4</sub> as Oxide:

With Si<sub>3</sub>N<sub>4</sub> as oxide, Drain Current versus Gate bias voltage is drawn. As the pH value is increased in the form change in the density of states, Drain current sees a shift in the Drain current same as SiO<sub>2</sub>. Drain voltage applied is similar to previous simulation at 100mV. Shift is little more than that of SiO<sub>2</sub> which can be proved with sensitivity achieved. Being high k oxide also helps in many other aspects such device performance remains stable over a long time. Change is observed mostly in the form of threshold voltage. This change in threshold voltage is proportional to sensitivity. Also pH characteristics shift to positive direction w.r.t SiO<sub>2</sub>. Maximum threshold shift observed is much more than that in case of SiO<sub>2</sub>. Sensitivity fluctuates for different pH, hence the sensitivity is measured as maximum change. For this case maximum sensitivity observed is 597mV.

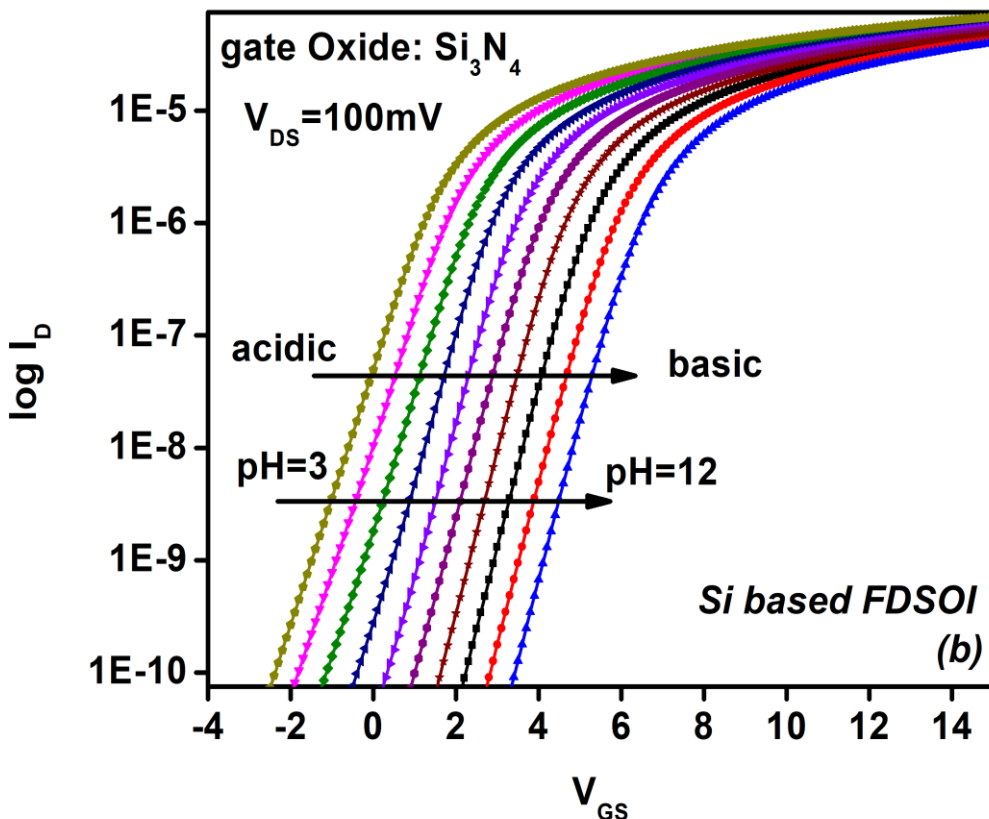


Fig 5.3 pH Sensing characteristics for Si<sub>3</sub>N<sub>4</sub>

### 5.2.3 Al<sub>2</sub>O<sub>3</sub> as Oxide:

Moving to Al<sub>2</sub>O<sub>3</sub> sees a much greater change in threshold shift w.r.t SiO<sub>2</sub>. Al<sub>2</sub>O<sub>3</sub> has been used in many sensors which has already proved its worth. It has been used in Biosensors such as cancer detection devices where it is known to have enhance the performance. For this case Drain voltage applied is similar to previous simulation at 100mV. Shift is little more than that of SiO<sub>2</sub> and Si<sub>3</sub>N<sub>4</sub> which can be proved with sensitivity achieved. Being high k oxide also helps in many other aspects such device performance remains stable over a long time. With rise in pH, Drain Current characteristics are similar to above but change is in the form of threshold voltage. Graph shifts to right as the solution changes from acidic to basic. Maximum threshold shift observed for this case is much higher than SiO<sub>2</sub> as oxide. Maximum sensitivity observed in this case is measured at 629mV.

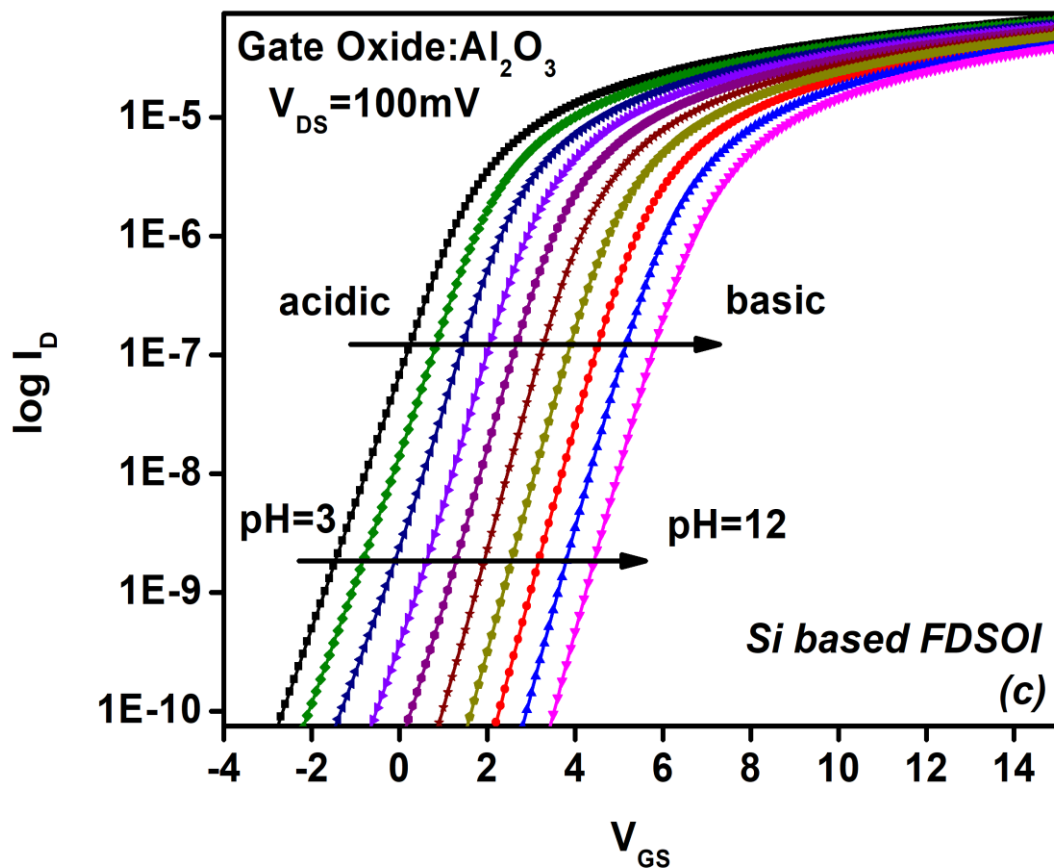


Fig 5.4 pH Sensing characteristics for Al<sub>2</sub>O<sub>3</sub>

### 5.3 Si versus SiGe:

The enhanced sensitivity using SiGe can be attributed to the enhancement in the sensing performance metrics i.e. the drain current and device transconductance [20]. Change in X composition of Germanium component in SiGe decides the performance of device in terms of threshold voltage and leakage current. If we increase the x composition Threshold voltage might increase but there is also increase in the leakage current. The optimum value for Si and Ge concentrations in  $\text{Si}_{1-x}\text{Ge}_x$  has been chosen as 0.5 to attain optimum device sensitivity along with leakage current. There is also considerable change in transconductance as shown and written below. Also SiGe shows fast response time since the current rises fast in case of SiGe rather than Si. The comparative analysis of device characteristics for conventional Si based FD-SOI and SiGe based device using  $\text{Al}_2\text{O}_3$  as gate dielectric is shown in Fig.5.5. The device drain current in SiGe based device ( $73\mu\text{A}$ ) is found to be improved over Si based device ( $55\mu\text{A}$ ) by 32.72%. Similarly when  $g_m$  is considered SiGe based device exhibits a higher  $g_m$  of  $6.68\text{mS/mm}$  which is 47.13% higher than Si based device ( $4.54\text{mS/mm}$ ).

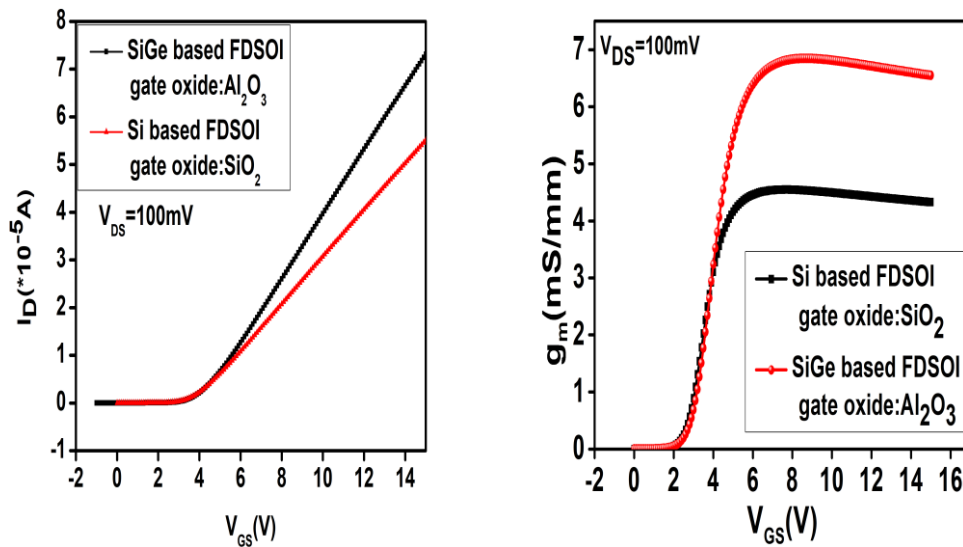


Fig.5.5. Comparison of device transfer and transconductance characteristics

Above two graphs support selection of SiGe over silicon. SiGe surpass silicon in terms of transconductance as well as sensitivity.

## 5.4 Results

### 5.4.1 Final FDOSI with Al<sub>2</sub>O<sub>3</sub> as Oxide:

Below is the final graph for SiGe based FD-SOI for Al<sub>2</sub>O<sub>3</sub> as gate oxide. Using Al<sub>2</sub>O<sub>3</sub> as oxide along with SiGe as channel material has further increased the sensitivity to a maximum of 760mV. Final device shows promising results with enhanced sensitivity. Results are shifted towards negative side w.r.t SiO<sub>2</sub>. Being high Sensitivity leads to better measurement of pH solution since the accuracy is increased. This increased sensitivity might help where we need to differentiate between very close pH solutions.

As the basicity is increased i.e solution is basic in nature output graph shifts into right direction. This shift is more than in earlier simulations. This result is supported by high sensitivity of 760mV for pH<sub>11</sub> to pH<sub>12</sub>.

Following Drain current characteristics is obtained.

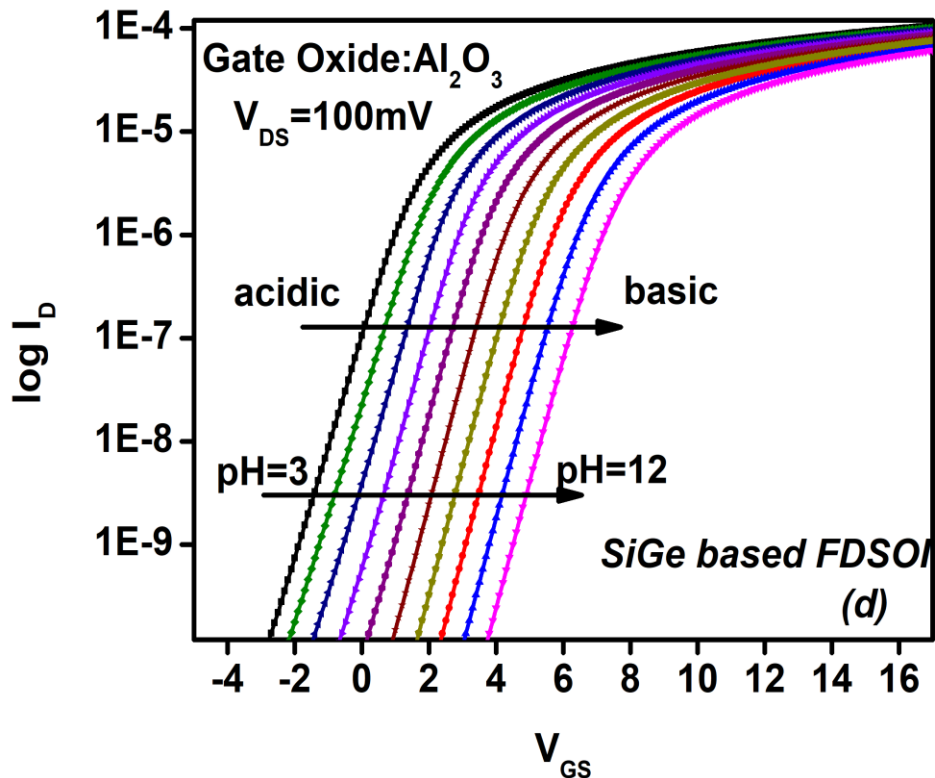


Fig 5.6 pH Sensing characteristics for SiGe based Device

### 5.4.2 Sensitivity Comparison:

The sensitivity of a basic Si based FDSOI and SiGe based proposed SOI with high-K  $\text{Al}_2\text{O}_3$  as gate dielectric is plotted in Fig.5.7. The device performance almost doubles when SiGe based proposed device is considered and the device sensitivity is found to linearly increase with the pH unlike the conventional device. The impact of pH immobilization on sensitivity has also been investigated for Si based devices with varying dielectrics.

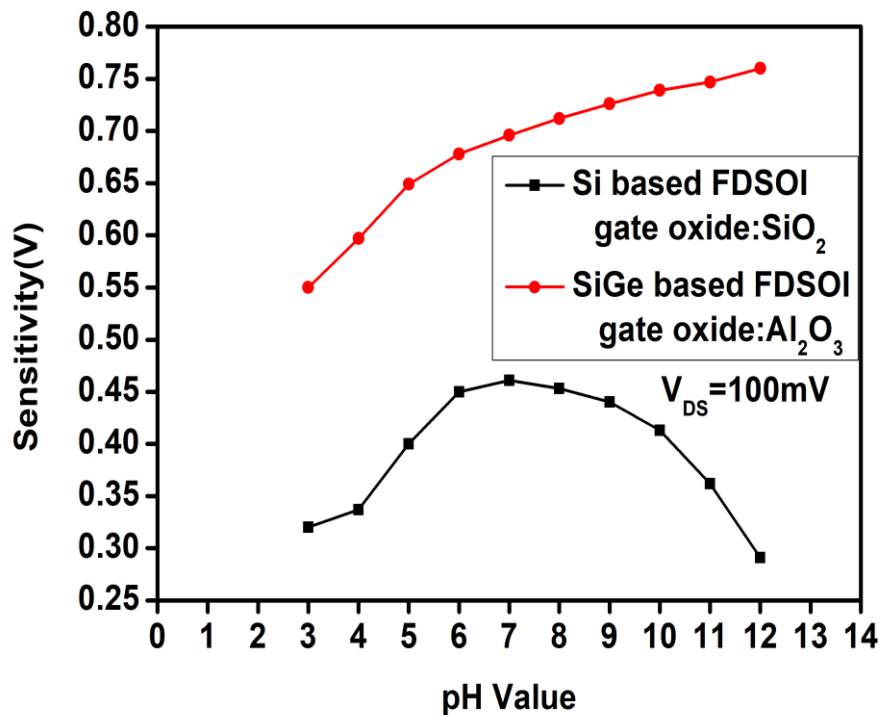


Fig. 5.7 Sensitivity enhancement of proposed device over conventional Si based device

When pH is shifted in the positive direction an equivalent linear current shift in positive direction is observed. In this analysis too, the  $\text{Al}_2\text{O}_3$  based devices outperforms the other dielectrics as the sensing current shifts are higher. Further with the dielectric variation the device transfer characteristics of  $\text{Si}_3\text{N}_4$  based SOI exhibits a positive shift with respect to  $\text{SiO}_2$  based device whereas  $\text{Al}_2\text{O}_3$  based device exhibits a shift towards the negative direction. The results for Si and SiGe based devices showing the best performance using  $\text{Al}_2\text{O}_3$  as dielectric is shown above results.

The drain current based sensitivity can be evaluated using the equation [20].

$$\Delta I_D \text{ sensitivity} = \left| \frac{I_{D1} - I_{D2}}{pH_1 - pH_2} \right| \quad \text{equ.}(5.2)$$

Sensitivity parameter can be expressed in following equation [19]:

$$\Delta V_{th} \text{ sensitivity} = \frac{V_{th}(pH_1) - V_{th}(pH_2)}{pH_1 - pH_2} \quad \text{equ.}(5.3)$$

### 5.5 Impact of pH Immobilization on Channel Potential

As the acidity of the electrolytic solution increases, as shown in Fig.8 the channel potential shows an upward shift. Fringing field lines, both inner and outer leads to the potentials that rise at the source-channel and the drain-channel interface. The channel potential drops from 0.073V to -0.2397V in the channel as shown in the figure. The variation in potential is seen to be 310mV when the pH of the electrolytic solution is varied from 2 to 10. It can be seen from the output that channel potential inside the channel remains almost same while the source and drain have elevated potentials. Potential is seen to decrease across the channel as we increase the pH.

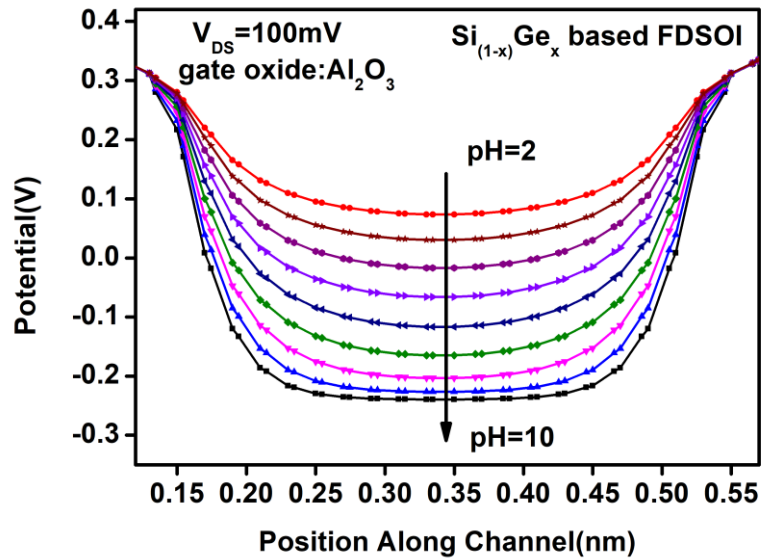


Fig. 5.8. Impact of pH immobilization on device channel potential

Potential shift shows how the potential is changing w.r.t pH change. This change also affects the threshold voltage at back gate.



## 5.6 Device Cut off Frequency

It can be concluded from the above analysis that the SiGe based device outperforms its Si based counterpart and best performance is showcased when  $\text{Al}_2\text{O}_3$  is used as the gate dielectric. The device response time is another parameter which has to be kept minimum when the device is used in sensing applications. Response time is similar to rise time. For better response time a device is supposed to have a less rise time.

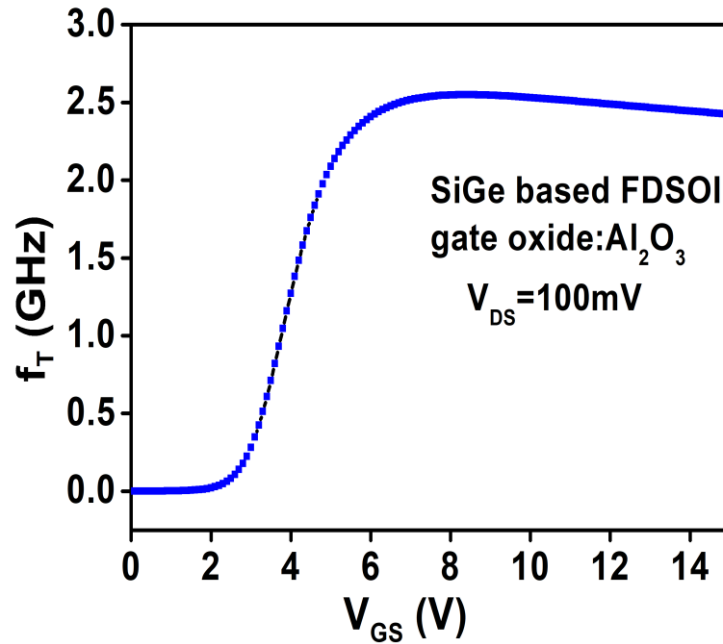


Fig 5.9. Cut off frequency of the proposed SiGe based pH sensor

This response time can be calculated with the help of unity gain frequency calculation. Unity gain frequency defines the frequency where the gain becomes one. It is advised to operate device under this frequency only. After unity gain frequency gain becomes less than one. Unity gain frequency can be calculated with the help of transconductance, gate to drain and gate to source capacitance with below given formula. Cut off frequency can be calculated as maximum frequency from unity gain frequency graph. So here the cut off frequency of the device is plotted in Fig.9. The high cut off frequency of 2.567 GHz ensures the fast response time of the device when used as a physical pH sensor.

This cut off frequency ( $f_T$ ) plotted has been attained using the equation[18]:

$$f_T = \frac{g_m}{2\pi(C_{GS} + C_{GD})}$$

Where  $g_m$  is the device transconductance,  $C_{GS}$ the gate to source capacitance and  $C_{GD}$  the gate to drain capacitance [18].

---

### Conclusion

High resolution pH detection has gained huge research focus over the past decade and there exists necessity of high sensitive pH sensors for detection of malignant tumors and other diseases from human blood. Proposed here is the sensitivity enhancement of an SOI based pH sensor where SiGe has been used as the channel. The overall performance evaluation of the device has been analyzed for various gate dielectrics and a comparative analysis has been presented of the proposed system sensitivity with the conventional device. Conventional device had a sensitivity of 450mV with SiO<sub>2</sub> as gate oxide. Device has been optimized first with optimum dimensions to achieve maximum sensitivity. Dimensions have also been optimized in order to minimize the leakage currents. Device has been simulated with different oxides such Si<sub>3</sub>N<sub>4</sub> and Al<sub>2</sub>O<sub>3</sub>. This resulted in further enhancement in sensitivity in terms of V<sub>th</sub>. But changing the material also had the opportunity to increase the sensitivity. With introduction of SiGe as channel material the sensitivity increased further more. With optimum value of x composition the sensitivity and leakage current was optimized. Usage of high k dielectric will also help in less degradation with over time. The proposed system outperforms the Si based device with an enhanced V<sub>th</sub> based sensitivity of 760mV/pH. Further for ensuring the fast response the device cut off frequency has been analyzed which evaluates to 2.56GHz.

### Future Work

pH measurement can act as an important parameter before starting any project with the solution. These projects take use of pH sensors according to their requirement. A some places we might require power saving sensors because of power limitation while other may require sensors with high sensitivity in order to get better accuracy. Future work can be done in designing the device more optimized. This optimization can in form of power saving. With usage of more suitable dielectric it might be possible to possible to reduce leakage current which act as a constant drainage outlet. These optimization can help into usage of devices at places where power supply is limited such as space missions.

## References

- [1]. S. Martinoia, G. Massobrio, and L. Lorenzelli "Modeling ISFET microsensor and ISFET-based microsystems: A review," *Sens. Actuators B, Chem.*, vol. 105, no. 1, pp. 14–27, 2005.
- [2]. A. Chandrakasan, B. Nikolic and J. M. Rabaey, *Digital Integrated Circuits*, New York: Pearson Education, 2003.
- [3]. S. Takagi, J. Koga and A. Toriumi "Subband structure engineering for performance enhancement of Si MOSFETs" *Int. Electron Devices Meeting Tech. Dig.* pp. 219-222 1997.
- [4]. M. Sshwarz, T.Holtij and A. Kloes "MOS: A New Physics-Based Explicit Compact Model for Lightly Doped Short-Channel Triple-Gate SOI MOSFETs," *IEEE Trans. on Electron Devices*, vol. 59, no. 2, pp. 349-358, 2012.
- [5]. F.Pregaldiny, N. Chevillion, C.Lallement and A. Yesayan "Physics-based compact model for ultra-scaled FinFETs," *Solid State Electronics*, vol. 62, no. 1, pp. 165-173, 2011.
- [6]. N. Mohankumar, B. Syamal and C. K. Sarkar "Influence of channel and gate engineering on the analog and rf performance of DG MOSFETs", *IEEE Trans. on Electron Devices*, vol. 57, no. 4, pp. 820-826, Apr., 2010.
- [7]. B. E. Deal, M. Sklar, A. S. Grove, and E. H. Snow "Characteristics of the surface state charge (QJ8) of thermally oxidized silicon," *J. Electrochem. Society* vol.114, pp. 266-274, March 1967.
- [8]. R. E. G. Van Hal, J. C. T. Eijkel, and P. Bergveld "A general model to describe the electrostatic potential at electrolyte oxide interfaces," *Adv.Colloid Interface Sci.*, vol. 69, no. 1, pp. 31–62, 1996.
- [9]. T.Poiroux, O. Faynot, C. Raynaud, C. Tabone, F. Allain and G. Reimbold "Interface coupling and film thickness measurement on thin oxide thin film fully depleted SOI MOSFETs" *ESSDERC '03. 33rd Conference on European Solid-State Device Research*, 2003.
- [10]. G. Tsutsui, M. Saitoh, T. Nagumo and T. Hiramoto "Impact of SOI Thickness Fluctuation on Threshold Voltage Variation in Ultra-Thin Body SOI MOSFETs" *IEEE Trans. on Nanotechnology* Vol. 4 ,Issue 2005
- [11]. Y.-J. Huang "High performance dual-gate ISFET with non-ideal effect reduction schemes in a SOI-CMOS bioelectrical SoC" *Proc. IEEE Int. Electron Devices Meeting (IEDM)* pp. 29.2.1-29.2.4 2015
- [12]. D. E. Yates, S. Levine and T. W. Healy "Site-binding model of the electrical double layer at the oxide/water interface" *J. Chem. Soc. Faraday Trans. 1 Phys. Chem. Condens. Phases* vol. 70 pp. 1807-1818 1974
- [13]. S. Koneshan, J. C. Rasaiah, R. M. Lynden-Bell and S. H. Lee "Solvent structure, dynamics, and ion mobility in aqueous solutions at 25 C," *J. Phys. Chem. B*, vol. 102, no. 21, pp. 4193–4204, 1998.
- [14]. H. J. Jang and W.J. Cho "Fabrication of high-performance fully depleted silicon-on-insulator based dual-gate ion-sensitive field-effect transistor beyond the Nernstian limit," *Appl. Phys. Lett.*, vol. 100, no. 7, pp. 073701-1–073701-4, 2012.
- [15]. *ATLAS User's Manual*, Silvaco, Santa Clara, CA, USA, 2013.
- [16]. <https://www.quora.com/>

- [17]. I.-Y. Chung, H. Jang, J. Lee, H. Moon, S. M. Seo, and D. H. Kim "Simulation study on discrete charge effects of SiNW biosensors according to bound target position using a 3D TCAD simulator," *Nanotechnol.*, vol. 23, no. 6, pp. 065202-1–065202-8, 2012.
- [18]. A. Bandiziol, P. Palestri, F. Pittino, D. Esseni and L. Selmi "A TCADbased methodology to model the site-binding charge at ISFET/electrolyte interfaces," *IEEE Trans. Electron Devices*, vol. 62, no. 10, pp. 3379–3386, Oct. 2015.
- [19]. Ajay, R. Narang, M. Saxena and M. Gupta "Analytical Model of pH sensing Characteristics of Junctionless Silicon on Insulator ISFET" *IEEE Trans. On Electron Devices*, vol. 64, no. 4, april 2017
- [20]. A. Varghese, C. Periasamy and L. Bhargava "Analytical Modeling and Simulation-Based Investigation of AlGaN/AlN/GaN Bio-HEMT Sensor for C-erbB-2 Detection," *IEEE Sens. J.*, vol. 18, no. 23, pp. 9595-9603, Dec, 2018.
- [21]. <https://allthingsvlsi.wordpress.com/>
- [22]. P. Fromherz, A. Offenhäusser, T. Vetter and J. Weis "A neuron-silicon junction: A retzius cell of the leech on an insulated-gate field-effect transistor," *Science*, vol. 252, no. 5010, pp. 1290–1293, 1991.
- [23]. <https://www.ques10.com>